USDI/USGS 08HQGR0103

Geometry, kinematics, and activity of a young mainland-dipping fold and thrust belt: Newport Beach to San Clemente, California

Authors: **Christopher C. Sorlien** (P.I.), **Brian A. Campbell**, and **Leonardo Seeber**

Sorlien: Institute for Crustal Studies (to become Earth Research Institute)
University of California, Santa Barbara
email: chris@crustal.ucsb.edu
Home office phone in Missouri: 573-447-0642

Campbell: Department of Geology, University of Missouri
campbell002@hotmail.com
Lab phone: 573-882-2884

Leonardo Seeber: Lamont Doherty Earth Observatory of Columbia University
nano@ldeo.columbia.edu
845-365-8385

Term of award: July 1, 2008 – June 30, 2009

ABSTRACT

Identification of the problem and implications

Contraction in southern California results in thrust slip on blind or partly blind faults beneath large complex anticlines (anticlinoria). The faults responsible for two regional folds adjacent to Los Angeles are not well-characterized and their activity is controversial. These structures are the Palos Verdes anticlinorium and the southwest-dipping fold limb that underlies the continental slope between Newport Beach and Oceanside. The Palos Verdes anticlinorium is a mainly offshore 70 km-long structure located immediately adjacent to Los Angeles. The dip direction, activity, and even existence of blind faults capable of forming the regional folds is controversial. The 2010 California Fault Activity Map shows discontinuous faults through much of our study area. Our new interpretation includes much more continuous faults, and a stratigraphic horizon that is an order of magnitude older than has been recently published.

Summary of Approach

Thousands of kilometers of industry and USGS seismic reflection data, constrained by well data, were used to create digital maps of near base Pliocene to early Quaternary horizons over 3000 square km of offshore southern California. Faults that deform the early Quaternary horizon were compiled. Bathymetric grids, incorporating multibeam and point data, were compiled. A 1D velocity model was used for depth conversion of the horizon surfaces and the San Mateo-Carlsbad fault surface. Fifty-eight cross sections were constructed and local strike, apparent dip, and structural relief measured and used for slip modeling.

Results

We interpret the right-lateral Newport-Inglewood fault to be part of a larger 3D system of oblique-right reverse faults. The NE-dipping San Mateo-Carlsbad fault projects downdip to intersect the Newport-Inglewood. Structural relief responds to bends in the fault consistently with a component of right-lateral slip that increases to the SSE. This fault bends sharply into a major releasing segment, with Quaternary separation flipping from reverse to normal across this bend. The system continues SSE as the Descanso fault onto the shelf just offshore of San Diego. Part of the slip is likely transferred farther across a right step to the Coronado Bank fault zone via a diffuse deformation zone. The Oceanside thrust from the SCEC Community Fault Model is reinterpreted to include 3 different fault strands. Most of the central strand does not deform the early Quaternary horizon, and has normal separation of the near base Pliocene horizon. Thus, the central segment is not a thrust and parts are not Quaternary-active. Its northwest end coincides with the San Mateo-Carlsbad fault and its southeast part coincides with the Coronado Bank fault. Progressive tilting in the hanging-wall above the northwest part of the San Mateo-Carlsbad fault and planar Quaternary angular unconformities now at between 500 m and 1200 m depth are consistent with regional subsidence. The Newport Beach-Oceanside slope and shelf (and San Joaquin Hills) are inverted Miocene basins relatively uplifting above the subsiding basin due to a thrust component of slip on the San Mateo-Carlsbad fault. The post-top Lower Pico (TLP, ~1.8 Ma +/-) dip-slip component of the upper few km of the northwest part of this fault is about 1 km. The post-TLP slip of the hanging-wall with respect to the footwall near the sharp bend is about 1 km towards the south and is locally pure right-lateral.

1: INTRODUCTION

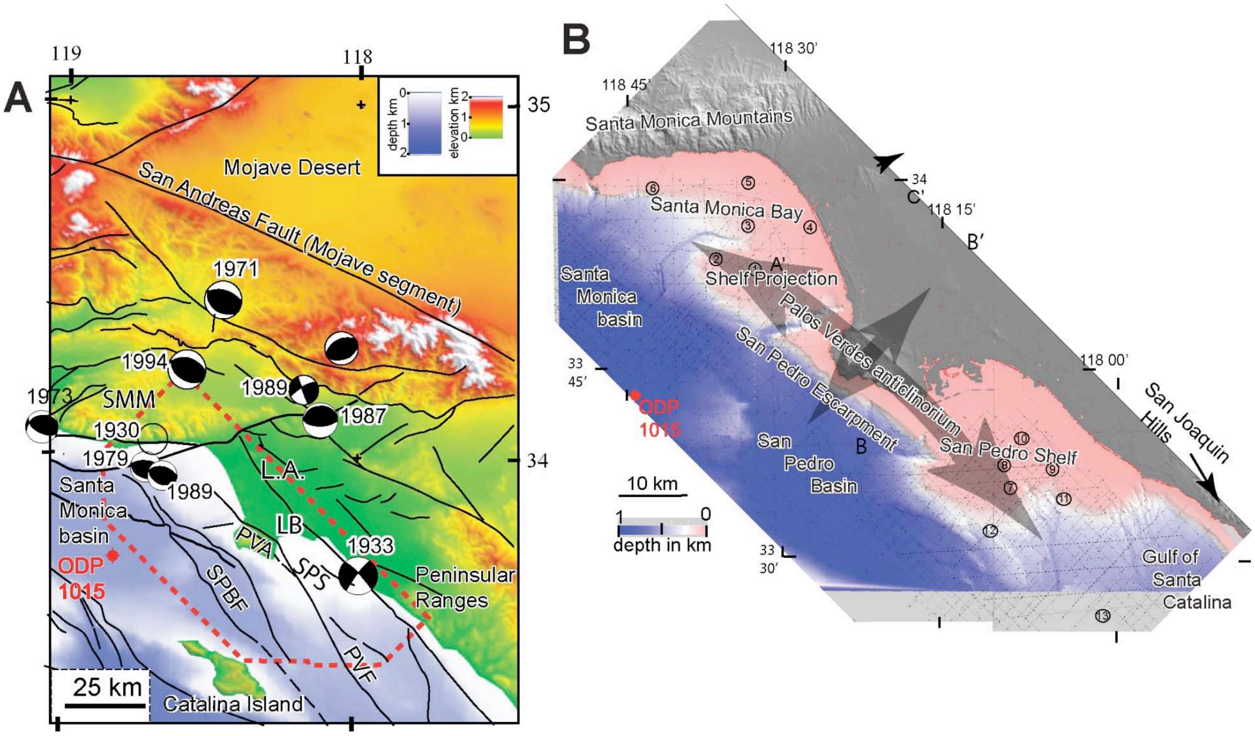

Figure 1: A) Faults and destructive earthquakes (USGS and SCEC, 1994). The traces or upper edges of blind faults are from the Southern California Earthquake Center Community Fault Model (Plesch et al., 2007) and from Sorlien et al.(unpublished manuscript). 1B is located by red dashed polygon. L.A.=Los Angeles (downtown); LB=Long Beach (city and harbor); PVA=Palos Verdes anticlinorium, PVF=Palos Verdes fault; SPBF=San Pedro Basin fault; SMM=Santa Monica Mountains; SPS=San Pedro Shelf). B) Multibeam bathymetry (Dartnell and Gardner, 1999) and SRTM topography, with tracklines of seismic reflection data (fine lines) and selected wells (numbered circles).

1.1: Anticlinoria and blind thrust faults

Along the southern California margin, mountains and submerged ridges are interpreted as the expression of anticlinoria, folded above blind thrust faults (e.g., Davis et al., 1989). Blind thrust faults have been the sources of several destructive southern California earthquakes, including the 1994 Northridge quake. The five km-deep Plio-Quaternary L.A. basin is isolated from other basins to the southwest by a 70 km-long anticline-ridge, the Palos Verdes Anticlinorium (PVA), (Fig. 1b; Davis et al., 1989; Shaw and Suppe, 1996; Broderick, 2006; Sorlien and Seeber, 2010 Sorlien et al. unpublished manuscript). The southwest limb of the PVA is expressed as the 700 m-high San Pedro sea floor escarpment (Fig. 1b). The southern part of this escarpment bounds San Pedro Shelf and gradually dies out southeastward (Fisher et al., 2004). Another 700 m-high sea floor escarpment bounding the narrow shelf between Newport Beach and Oceanside is also the surface expression of a regional southwest-dipping fold limb. It is underlain by the San Mateo-Carlsbad fault (Ryan et al., 2009), the northwest part of which coincides with the northwest part of the Oceanside thrust of Rivero et al., (2000). This fault segment is a reactivated Miocene low-angle normal fault (Crouch and Suppe, 1993). The actively uplifting San Joaquin Hills (Fig. 1B) are in the hanging-wall of this fault (Grant et al., 1999, 2002).

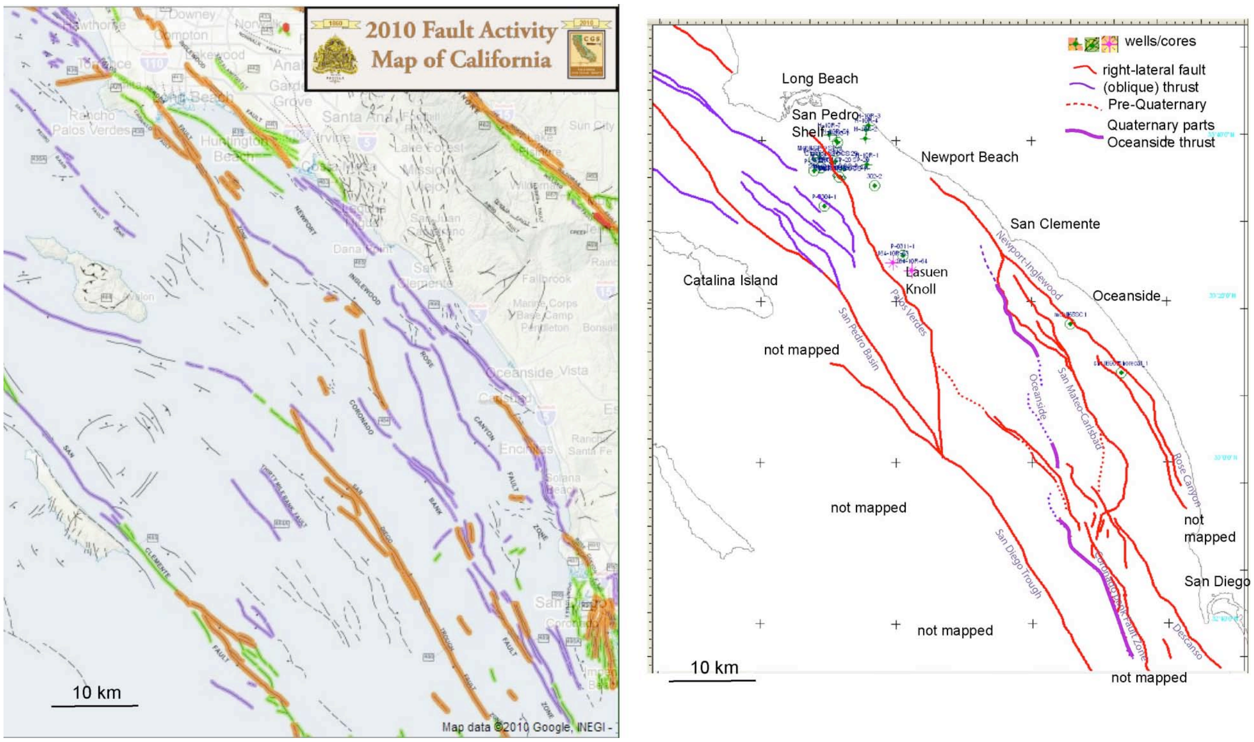

Figure 2: (left): A clip from the 2010 Fault Activity Map of California (Jennings et al., 2010). (right): Our map of Quaternary faults (solid lines) and just a couple examples of Pliocene faults (dashed), of the same area at the same scale. Blind faults are represented at their upper edges. Red faults are right-lateral and violet faults are (oblique) thrust.

Southern California is, of course, part of a dextral transform plate boundary. Many of the faults in the offshore study area are indeed right-lateral. Anticlines forming sea floor knolls may be associated with restraining segments of these faults. The larger limbs of anticlinoria are likely associated with oblique right-reverse slip, with partitioning or partial partitioning of slip between steep strike-slip faults and gently-dipping (oblique) thrust faults.

1b: Previous Structural Models for Palos Verdes Anticlinorium and San Joaquin Hills
One set of models explains the visible, uplifting part of the PVA as due to oblique right-reverse slip along a restraining segment of the Palos Verdes fault (e.g., Ward and Valensise, 1994). Alternatively, thrust slip on a SW-dipping roof thrust above a SW-directed tectonic wedge has been interpreted as the cause of folding and uplift of the PVA (Davis et al, 1989; Shaw and Suppe, 1996). We have proposed a variation of the regional thrust model, where a SW-dipping roof thrust is not required and (oblique) thrust slip reactivates NE-dipping faults that root beneath Los Angeles basin (Sorlien and Seeber, 2010).

Uplift of the San Joaquin Hills has been published as due to slip on an inferred blind SW-dipping (Fig. 1B; Grant et al., 1999, 2002; Grant and Shearer, 2004). However, such an interpretation does not explain uplift of the outer shelf on the opposite side of parts of the Newport-Inglewood fault relative to the subsiding Gulf of Catalina (San Pedro) basin. The NE-dipping blind Oceanside thrust is part of the Southern California Earthquake Center Community fault model (SCEC CFM), but is not part of California hazard models. If the northwest part of this fault is indeed a Quaternary thrust fault, its slip could explain the relief between the shelf and the basin.

The 2010 California Fault Activity Map shows discontinuous (dashed) faults through much of our study area (Jennings et al. 2010). Another new fault map benefited from use of much newly-

released industry seismic reflection data. This map also represents certain faults as discontinuous (Ryan et al., 2009). Published structure-contour maps of Neogene stratigraphic horizons that incorporate interpretation of the newly-released industry seismic reflection data do not exist for the offshore between Long Beach and San Diego. Recent publications that extrapolate below radiocarbon dating range interpret submarine fan deposits to mostly date from Oxygen Isotopic Stage 6 and later (~160 ka)(Covault and Romans, 2009; Normark et al., 2009).

Our new fault, fold, and stratigraphic interpretation differs from what has been published between 2007 and present. In particular, we interpret more continuous faults and interpret a shallow regionally-mapped horizon to be an order of magnitude older than published by Covault and Romans, (2009) and Normark et al. (2009).

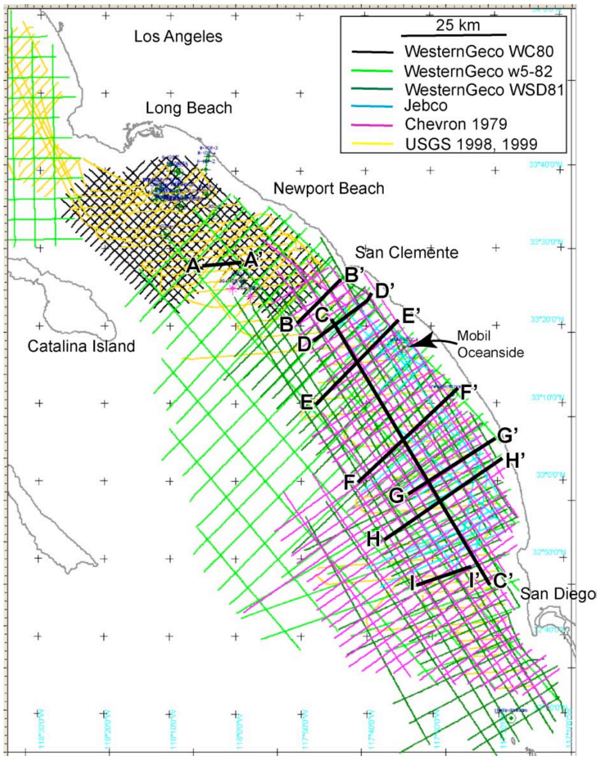

Figure 3: Tracklines of migrated seismic reflection profiles used in this study. Additional data were used in the area northwest of Long Beach, shown as faint lines in Fig. 1b. Figures showing profiles are located, with the exception of Figure 15. 3500 trackline km were interpreted for the area of the northern half of this map for past SCEC-funded projects, with a similar amount of data added for this study (south half).

2: DATA

Much offshore southern California industry seismic reflection data (from Western Geophysical, Chevron, and Jebco) are available online (http://walrus.wr.usgs.gov/NAMSS/index.html). USGS migrated multichannel seismic reflection profiles acquired in 1998 and 1999, using a small airgun and 250 m streamer, are also available online (Fig. 3; Sliter et al., 2005; http://pubs.usgs.gov/of/2005/1084/data_tables.html). Multibeam and point bathymetric data were available for Dartnell and Gardner (1999), and the National Geophysical Data Center: http://www.ngdc.noaa.gov/mgg/bathymetry/multibeam.html
http://www.ngdc.noaa.gov/mgg/bathymetry/hydro.html

Stratigraphic data provide the age control needed to examine evolution of faults and folds. Well data for petroleum test wells were found at the Long Beach office of the California Division of Oil and Gas, in files held at UCSB, and especially from the U.S. Minerals Management Service (MMS), which made available about 25,000 logs from offshore west coast wells, as well as their paleontological reports. These logs are being made available online by the U.S. Geological Survey. Shallow cores with paleontology were used by Nardin and Henyey, (1978) to create maps of sea floor outcrop (also Vedder, 1990). We also made use of published cross sections that extend

offshore (Wright, 1991), logs from wells on San Pedro Shelf (Fig. 1B), and stratigraphic information from Rigor (2003). Checkshot and sonic velocity surveys were used for certain wells.

3: METHODS

3.1 Digital representations stratigraphy and faults

The interpretation was performed using an interactive industry seismic reflection and well interpretation software, "The Kingdom Suite". The industry and USGS seismic reflection data shown in Figure 3 were loaded into a Kingdom Suite interpretation project. Bathymetric grids were created with assistance from Marie-Helene Cormier, and converted to two-way travel time using an interval velocity of 1490 m/s. The bathymetry could then be displayed on the seismic reflection profiles so that the seismic trace - navigation correspondence could be adjusted for two surveys (The WesternGeco w5-82 data and the Chevron data; Fig. 3). The shot number in the SEGY headers of the Chevron does not exist or does not correspond to the text navigation file. The correspondence between trace number and navigation for the w5-82 survey depends on which direction the profile was shot, and even after one figures that out, many of the profiles require a 10 or 20 shot shift of one end of the profile. Sub-bottom structure was interpreted together with the bathymetry. Well data were also incorporated into the Kingdom Suite project.

The well and sea floor outcrop information was converted to travel time and correlated through the grids of reflection data using loop-tying techniques, accounting for vertical and horizontal shifts resulting from 2D migration of dipping strata. This was the most difficult and time-consuming part of the project, requiring expertise and precision. Base "Repetto" (~4.5 Ma, same as top Delmontian benthic foraminiferal stage), top "Repetto" (~2.5 Ma), and top Lower Pico (~1.8 Ma) horizons (Blake, 1991) were extended from our existing interpretation of San Pedro Shelf and slope to south of Lasuen Knoll (Fig. 2). Onlap and other pinchouts precluded correlation of top and base Repetto to the south via eastern paths, and base Repetto partially merged with older rocks along the western correlation paths. A reflection, H4 (blue) was chosen beneath the

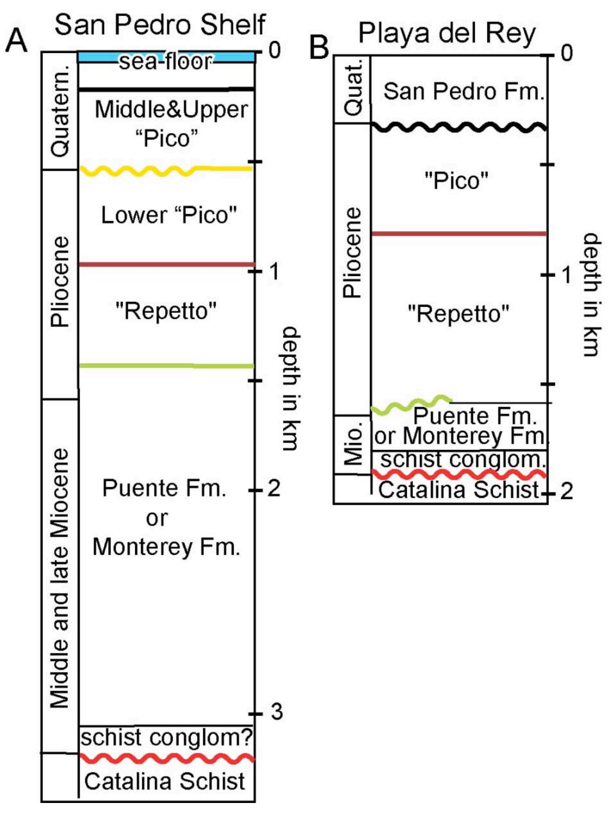

Figure 4: Stratigraphic columns. Colors show our interpreted horizons, wavy lines are unconformities. H4 (blue) approximately correlates to Base Repetto. A: From San Pedro Shelf, on the downthrown side northeast of the Palos Verdes fault (redrawn from Wright, [1991]). B: Depths from the Playa del Rey field, except San Pedro Formation, which may be late Quaternary. B: is from the nearby offshore Venice field, located due west of downtown Los Angeles. From Sorlien et al. [2006], drawn from California Div. Oil and Gas [1992].

Gulf of Santa Catalina and correlated regionally. It is younger than late Miocene strata identified near the top of the Mobil Oceanside well (Fig. 3; Crouch and Suppe, 1993), and approximately correlates to base Repetto (~4.5 Ma).

Gently-to moderately dipping faults are directly imaged because the contrasting velocities and densities across them produce strong fault-plane reflections. Other criteria for fault interpretation include the relationship of stratal folding to fault plane reflections, and truncations or offsets of stratal reflections.

3.2 Gridding and Depth Conversion

Time-depth charts at wells, using sonic logs and check-shot surveys, were used to convert geologic information to two-way travel time for wells on San Pedro Shelf and for the Mobil Oceanside well. The interpretation and gridding of two stratigraphic horizons and one fault was then done in two-way travel time. Grids were converted from time to depth using the water layer and a function of linearly increasing interval velocity with respect to sub-sea floor depth. This is the linear velocity equation, with constants appropriate for the California margin (Tolmachoff, 1993), for depth conversion. The sea floor velocity used was 1500 m/s and the constant was 0.6. Although 1500 m/s is slow where pre-latest Quaternary strata outcrop, a velocity survey gives similar slow velocity for well 304 #1 on San Pedro Shelf for late Pliocene strata just below the sea floor. Depth conversion was done within "The Kingdom Suite" using the extended math calculator.

Gridding was done using the shareware SURFACE III, using the projection of slopes technique (http://www.kgs.ku.edu/Tis/surf3/surf3Home.html). The point distribution of many data points along profiles and, in places, large distances between profiles are unfavorable for this type of gridding. Therefore, we skipped traces on the data export so that data points were spaced at about 100 m along profiles (rather than 5, 12.5, or 25 m of the trace spacing). A 500 m grid was done, exported, added together with the original import file, and regridded at 100 m. The resulting grid has few significant artifacts and matches the interpretations along profiles precisely. Most of the roughness of the H4 (blue) grid is due to numerous small faults, etc, and is not artifacts. The top Lower Pico (TLP) exported horizon text file was added to additional files of horizons interpreted on older strata where TLP onlaps, or along the sea floor where TLP outcrops. The H4 grid exists only where the horizon is distinct and present. Fault interpretations exported from "The Kingdom Suite" include only those points that were digitized, and we digitized points to be relatively equally spaced on profiles. The San Mateo-Carlsbad fault was gridded at 400 m, exported, and the 400 m grid regridded at 100 m (without recombining with the original file).

4: **RESULTS AND DISCUSSION**

4.1: **Fault Geometry**

Figures 2, 5, and 6 illustrate the fault and fold pattern of the study area. Our maps place the fault traces at their upper edge, which is near the seafloor for young active strike-slip faults, and in the deeper sub-bottom for blind or buried faults. The 2010 Fault activity map of California (Jennings et al., 2010) is very similar to the 1994 map (Jennings, 1994), and likely did not include studies with access to voluminous deep industry multichannel seismic reflection data (Fig. 2A). Our fault pattern differs from that of Ryan et al. (2009). Ryan et al. (2009) focused on Holocene-active faults, and presumably mapped faults in the shallow sub-bottom. We mapped the more important faults and a subset of smaller faults that deform the near-base Pliocene horizon. Faults that deform the early Quaternary top Lower Pico are shown as solid curves on our figures. This deformation can be by folding with the fault tip being below the horizon (blind fault, not buried fault). Certain faults, including the San Mateo-Carlsbad, are blind and were mapped on the lowest strand that deforms TLP. At depth, these faults are more continuous than the sometimes complex and discontinuous hanging-wall strands that cut closer to the sea floor. We used more industry data in our interpretations than were available to Ryan et al. (2009).

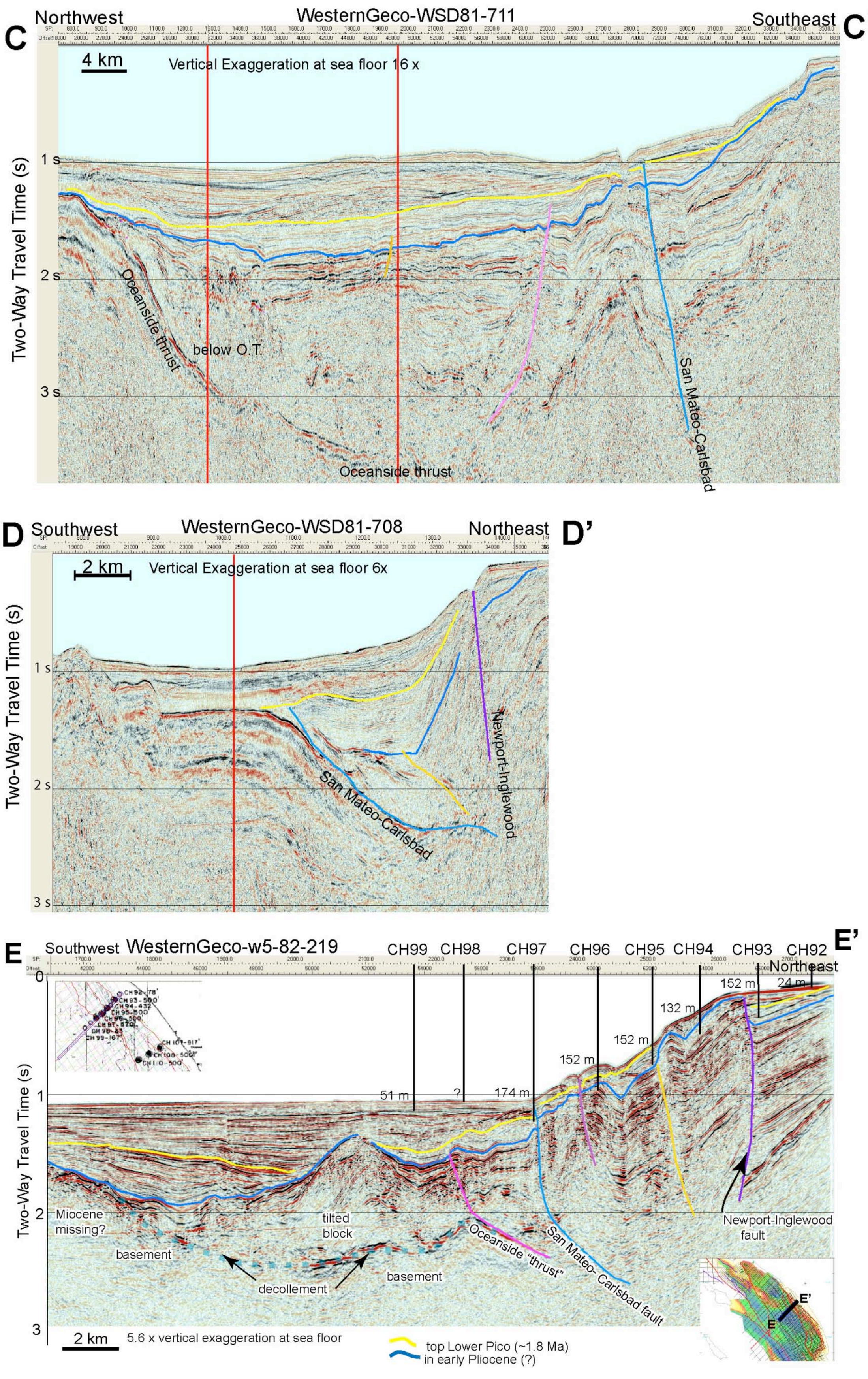
C
Northwest
WesternGeco-WSD81-711
Southeast
C'
4 km
Vertical Exaggeration at sea floor 16 x
Two-Way Travel Time (s)
1 s
2 s
3 s
Oceanside thrust
below O.T.
Oceanside thrust
San Mateo-Carlsbad
D
Southwest
WesternGeco-WSD81-708
Northeast
D'
2 km
Vertical Exaggeration at sea floor 6x
Two-Way Travel Time (s)
1 s
2 s
3 s
Newport-Inglewood
San Mateo-Carlsbad
E
Southwest
WesternGeco-w5-82-219
CH99
CH98
CH97
CH96
CH95
CH94
CH93
CH92
E'
Northeast
Two-Way Travel Time (s)
0
1
2
3
152 m
24 m
132 m
152 m
152 m
51 m
?
174 m
Miocene missing?
tilted block
basement
decollement
basement
Oceanside "thrust"
San Mateo- Carlsbad fault
Newport-Inglewood fault
2 km
5.6 x vertical exaggeration at sea floor
top Lower Pico (~1.8 Ma)
in early Pliocene (?)
E'
E

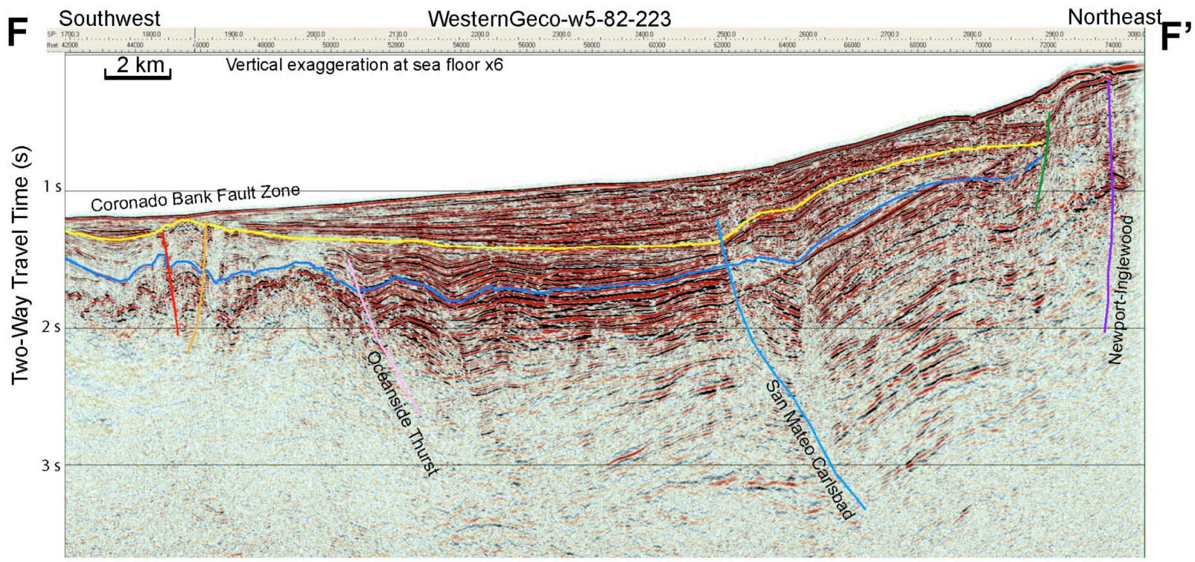
F
Southwest
WesternGeco-w5-82-223
Northeast
F'
2 km
Vertical exaggeration at sea floor x6
Two-Way Travel Time (s)
1 s
2 s
3 s
Coronado Bank Fault Zone
Oceanside Thrust
San Mateo-Carlsbad
Newport-Inglewood

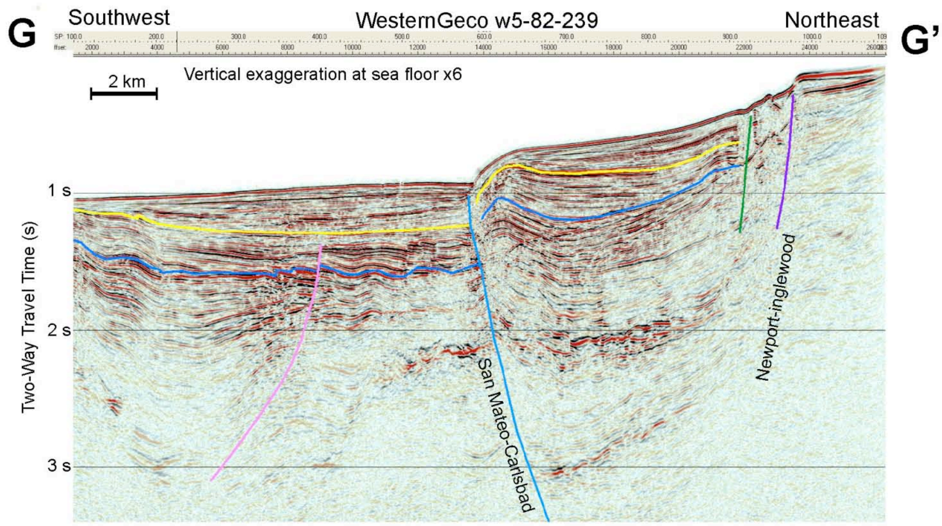
G
Southwest
WesternGeco w5-82-239
Northeast
G'
2 km
Vertical exaggeration at sea floor x6
Two-Way Travel Time (s)
1 s
2 s
3 s
San Mateo-Carlsbad
Newport-inglewood

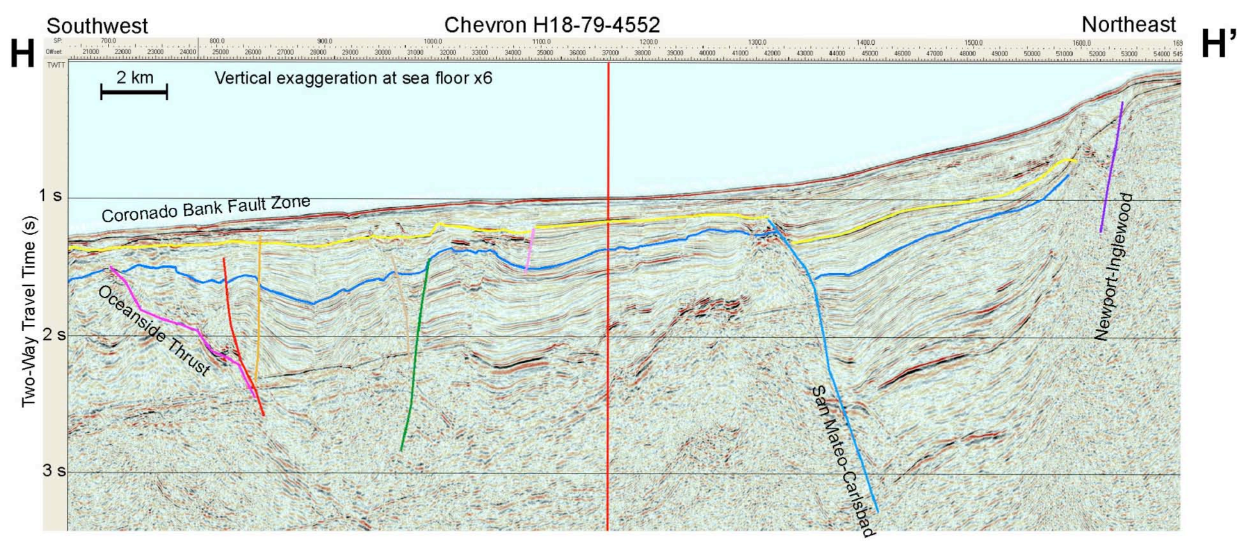
H
Southwest
Chevron H18-79-4552
Northeast
H'
2 km
Vertical exaggeration at sea floor x6
Two-Way Travel Time (s)
1 s
2 s
3 s
Coronado Bank Fault Zone
Oceanside Thrust
San Mateo-Carlsbad
Newport-Inglewood

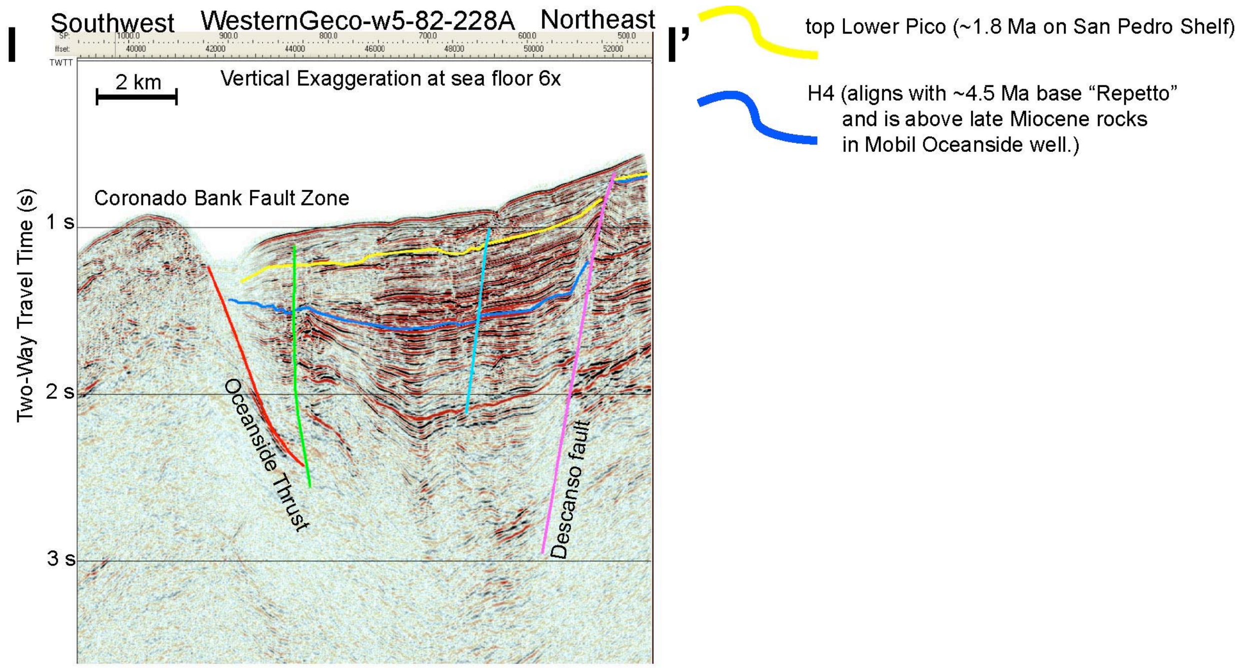

Figure 5: (above and previous pages): Interpreted industry seismic reflection profiles, located on Figure 3. C-C′ has three times the vertical exaggeration of the other profiles. The top row is shotpoint; the second row is meters along profile. **C**-C′ is one of our reference correlation profiles. It is mostly in the footwall of the San Mateo-Carlsbad fault but in the hanging-wall of a mostly inactive upper part of the Oceanside "thrust", which here is mainly a Miocene low-angle normal fault (possibly the Oceanside fault of Bohannon and Geist 1998; see Crouch and Suppe, 1993). **D – D′:** Oceanside thrust of Rivero et al. (2000) coincides with our San Mateo-Carlsbad fault. **E-E′:** A Miocene low-angle normal fault system dips northeast beneath the shelf and slope. It is reactivated, with slip being incompletely partitioned between the right-lateral Newport-Inglewood fault and the oblique right-reverse San Mateo-Carlsbad fault (Ryan et al., 2009; Campbell et al., 2009). Dashed cyan is a Miocene extensional decollement responsible for tilting of the labeled block. The along-strike Mobil Oceanside well indicates that the imaged sedimentary section near the Newport-Inglewood fault down to at least 1.5 s two-way travel time is Miocene. The shallow basement beneath the basin leaves little room for Miocene, and thus the slope and shelf is an inverted Miocene basin. We do not yet have access to the proprietary Caldrill 68 coreholes that are shown. U.S.G.S. employees may have the right to what data exist in U.S. Minerals Management files. **F-F′:** Here the Oceanside "thrust" does not significantly deform the top Lower Pico (yellow) and has normal separation on the near base Pliocene H4 (blue). There is no evidence for blind thrust slip beneath the central part of this profile because there is no Quaternary folding in between the Oceanside "thrust" and the San Mateo-Carlsbad fault**. G-G′**: Folding just above the tip of the San Mateo-Carlsbad fault is more pronounced than is the case on F-F′. This is related to double bends that are releasing and restraining for a component of right-lateral slip. **H-H′:** from here to the offshore Mexican border the Oceanside thrust coincides with the Coronado Bank fault zone of Legg (1991)/ the Coronado Bank Detachment of Nicholson et el.(1993, 1996). The San Mateo – Carlsbad fault is crossed near the northern bend of a releasing segment, with normal separation being consistent with right-lateral slip**. I-I′:** The San Mateo – Carlsbad fault is mostly truncated by/merges with the northwestern continuation of the Descanso fault of Legg et al., (1991).

The 60 km-long NNW-striking segment of the San Mateo-Carlsbad fault displays a gentle to moderate dip to the ENE (Fig. 5). Quaternary horizons exhibit a varying degree of reverse separation across this segment, though underlying Miocene horizons display normal separation. South of this segment, the fault bends 70 degrees, stepping right (releasing) by 9 km, and merges with the NNW-striking Descanso fault that continues towards Mexican territory across the shelf west and south of San Diego. This releasing segment and mapped fault strand represent an additional 55 km length. Right lateral slip may step right from the Rose Canyon fault in San Diego to the Descanso fault (M. Legg, electronic communication, May 03, 2010). A diffuse zone of many minor faults connects an additional 7 km across a right (releasing) step to the shallow parts of the Coronado Bank Miocene detachment fault (Coronado Bank fault zone, western part, of Legg, 1991). Near the 70 degree bend of the San Mateo-Carlsbad fault, Quaternary separation shifts abruptly from reverse to normal, and faults within the releasing stepover display consistent normal separation of the top Lower Pico and H4 Quaternary and Pliocene horizons (Fig. 5(H-H'), Fig. 6),). In addition to that major right stepover, more subtle bends characterize the NNW-striking segment. Overall, the deformation along the fault is typical of a moderately dipping oblique right lateral-reverse fault, showing reverse structural relief in the left-stepping bends and exhibiting subdued relief near right-stepping bends. Evidence for at least a component of right-lateral slip on the San Mateo-Carlsbad fault implies incomplete partitioning of right-lateral motion between it and the Newport-Inglewood fault in its hanging-wall. The shallow parts of these two faults merge near San Clemente (Fig. 6), and the Newport-Inglewood fault has a WSW-verging reverse component northwest of there in its offshore part. Preliminary interpretation of thickness variations between the top Lower Pico and near base Pliocene horizons suggests that transpressional folding initiated during Pliocene time in the hanging-wall of the San Mateo-Carlsbad fault, synchronous with transtension in the footwall basin.

The Oceanside thrust of Rivero et al. (2000) is included in the SCEC Community Fault Model (Plesch et al., 2007). Initially, we exported the Oceanside thrust from the SCEC CFM using Gocad, and imported this depth grid as a time object into Kingdom Suite. We displayed the Oceanside fault depth grid on the seismic profiles, and, accounting for the depth-time differences, interpreted the Oceanside thrust on the nearest significant fault. Where the SCEC CFM fault representation jumped between shallow faults strands, we re-interpreted the Oceanside thrust as having separate segments. Presumably, we are using much more abundant industry seismic reflection data than would have been available to Rivero et al. (2000). The southern part of the Oceanside thrust coincides with the western part of Coronado Bank fault zone (H-H' and I-I' in Fig. 5, Fig. 6; Legg, 1991; Nicholson et al., 1993). The northern part coincides with the northwest part of our San Mateo-Carlsbad fault (The San Mateo fault of Ryan et al., 2009)(D-D' in Figure 5). Parts of the central segment of the Oceanside thrust do not deform top Lower Pico and have normal separation of our H4 near base Pliocene horizon (F-F' in Fig. 5). A regional anticline expected due to deeper blind thrust slip on the Oceanside thrust beneath the Gulf of Santa Catalina is lacking (F-F' in Fig. 5). Adjoining faults with north strikes are right-lateral. Thus, the central part of this fault is not a thrust and is not a Quaternary fault.

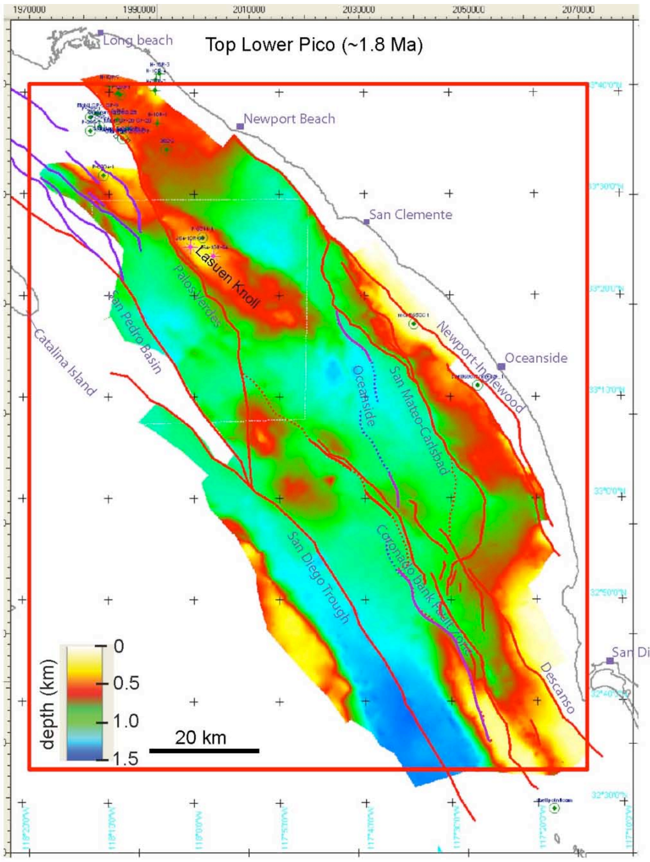
Top Lower Pico (~1.8 Ma)
Long beach
Newport Beach
San Clemente
Oceanside
San Diego
Lasuen Knoll
Palos Verdes
San Pedro Basin
Catalina Island
Oceanside
San Mateo-Carlsbad
Newport-Inglewood
San Diego Trough
Descanso
depth (km)
0
0.5
1.0
1.5
20 km

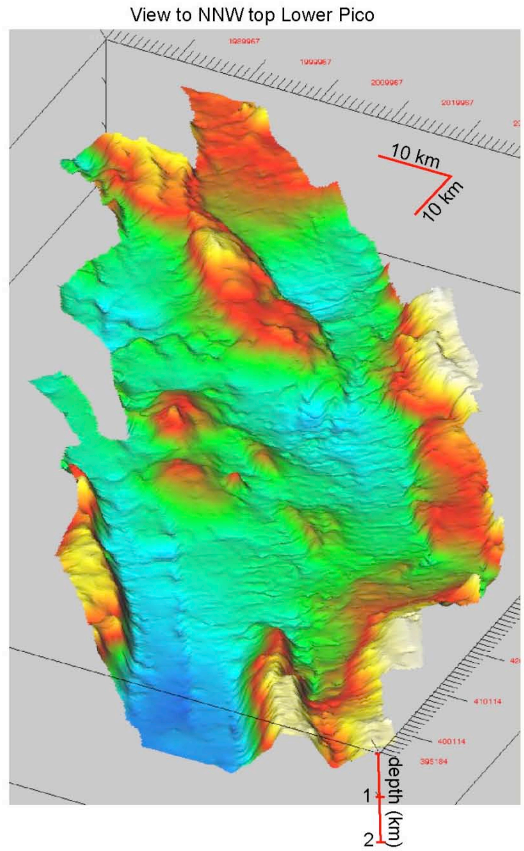
View to NNW top Lower Pico
10 km
10 km
depth (km)
1
2

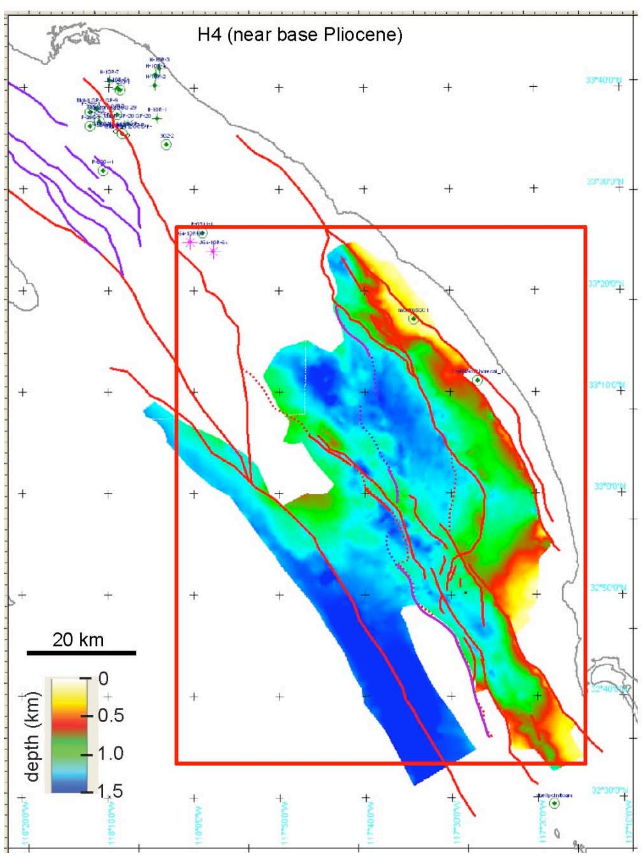
H4 (near base Pliocene)
20 km
depth (km)
0
0.5
1.0
1.5

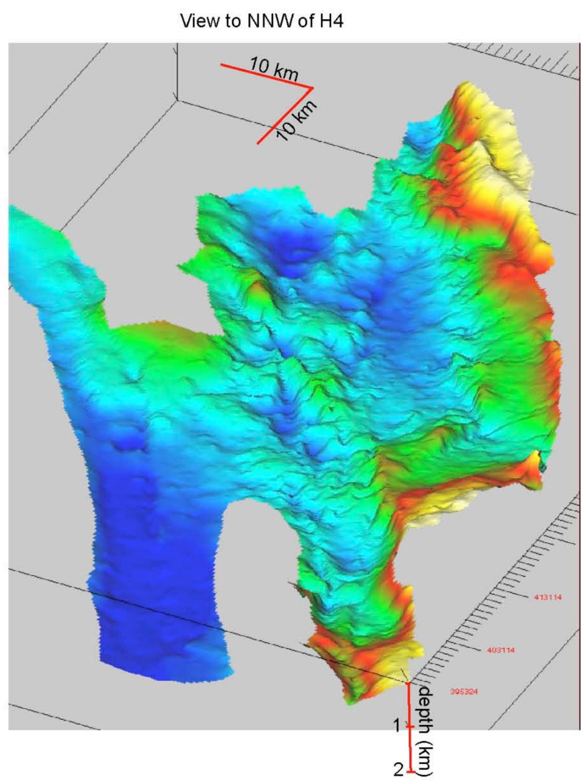
View to NNW of H4
10 km
10 km
depth (km)
1
2

Figure 6: (previous page): Plan views (left) and oblique views to the north-northwest of depth-converted 100 m grids of ~1.8 Ma top Lower Pico (TLP; top) and the near base Pliocene H4 (bottom). These grids were produced from interpretation of several thousand kilometers of migrated multichannel seismic reflection data, shown in Fig. 3. The TLP grid include older horizons where it onlaps, and sea floor where it outcrops. The near base Pliocene grid only includes areas were this horizon is present and distinct.

The Palos Verdes fault is interpreted to terminate near Lasuen Knoll by Brankman and Shaw (2009) and Ryan et al. (2009)(Fig. 6). Our digital horizon maps do not reveal transverse folds or extension that could absorb the more than 5 km of post-Miocene right slip proposed by Brankman and Shaw (2009) on San Pedro Shelf near the previously proposed southern termination of the PVF. No significant through-going faults are imaged that could carry such slip southeastward. Instead, the Palos Verdes fault bends to the south and connects to the San Diego Trough fault (Fig. 6; Alward et al., 2009). This newly-mapped releasing segment is associated with up to a 3 km-wide zone of normal-separation faults, especially near the northern bend. This fault segment is locally buried beneath about 200 m of unfaulted Quaternary sedimentary rocks and thus the least astonishing interpretation is that this segment is not active (Conrad et al., 2008; J. Conrad oral communication, October 30, 2009). A complex fault-fold trend connects the Palos Verdes fault to the Coronado Bank fault zone (e.g., Legg, 1991; Fig. 6). However, there is no continuous sea floor fault strand to complete the connection, and the northern part of this trend may also be buried. While part of the long-term right slip likely connects to San Diego Trough and the Coronado Bank fault zone, it remains unclear what happens to the >3 mm/yr of Holocene right-lateral slip measured at Los Angeles Harbor (Long Beach)(McNeilan et al., 1996). Perhaps slip is transferred to the east by clockwise rotation of the Lasuen Knoll block. The majority of young slip on the San Diego Trough fault continues north on the San Pedro Basin fault (Alward et al., 2009; J. Conrad oral communication, October 30, 2009).

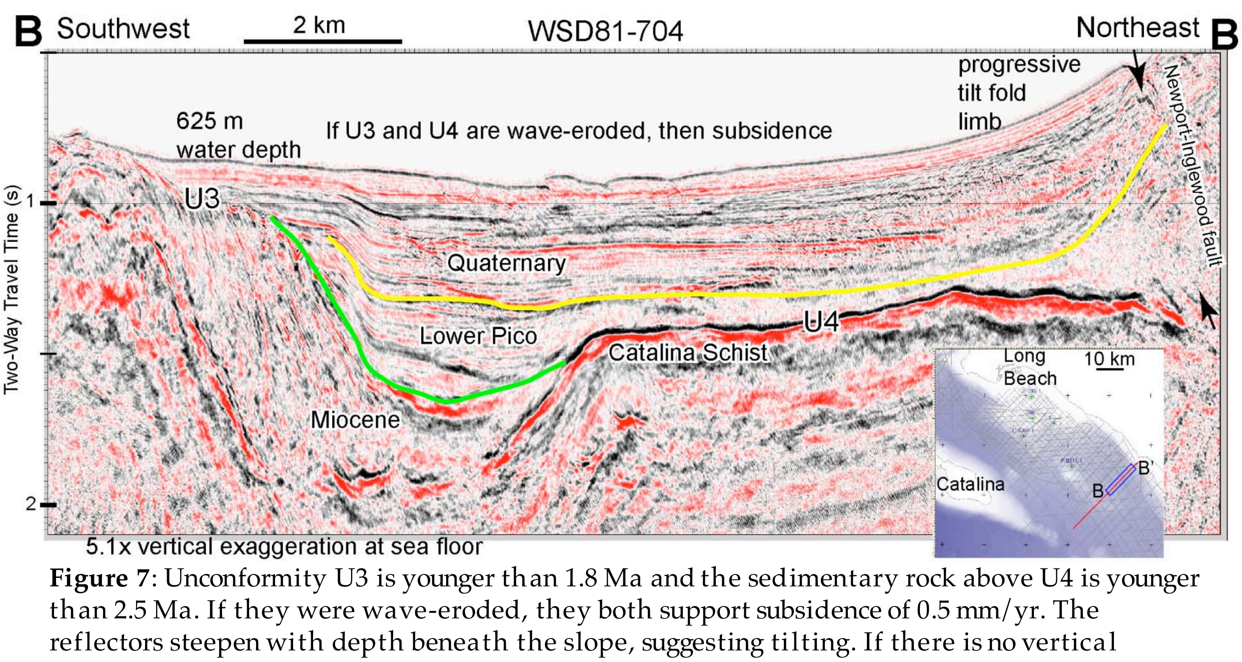

Figure 7: Unconformity U3 is younger than 1.8 Ma and the sedimentary rock above U4 is younger than 2.5 Ma. If they were wave-eroded, they both support subsidence of 0.5 mm/yr. The reflectors steepen with depth beneath the slope, suggesting tilting. If there is no vertical motion of the shelf, the basin must subside given tilt.

We did not generally attempt to interpret Miocene faults unless they have reactivated and substantially deformed Quaternary strata. Low-angle Miocene normal faults are pervasive and likely affect the kinematics and deep geometry of young faults, and thus affect seismic hazard.

4.2: Ongoing basin subsidence paired with active growth of anticlinoria

The Palos Verdes anticlinorium (PVA) is a regional NW-trending 70 km-long post-Miocene growth structure (Fig. 1B). It implies an underlying thrust-fault system of similar dimensions. Similarly, the southwest-dipping fold limb beneath the continental slope between Newport Beach and Oceanside extends ~100 km in the hanging-wall of the Newport-Inglewood fault (north) and San Mateo-Carlsbad fault. The Santa Monica and Los Angeles Basins have subsided respectively 4 km and 5 km in the last 5 m.y., and this subsidence probably continued through Quaternary time (Wright, 1991; Sorlien et al., 2006; Ponti et al., 2009). If the basins are simply marking regional lithospheric subsidence, then structural growth of the PVA and of the continental slope offshore San Clemente must be correspondingly rapid to keep the top of these structures near sea level (see Pinter at al. 2003). Figure 7 shows a pair of erosion surfaces where deposition did not resume until after 1.8 Ma, and until after 2 to 2.5 Ma respectively. If these are wave-eroded surfaces, then they have subsided respectively 0.6 and 0.9 km. The younger erosion surface is also imaged on many seismic profiles about 20 km to the northwest (Fig. 8). Additional unconformities just above top Lower Pico are seen at depths exceeding 1 km beneath the Gulf of Santa Catalina.

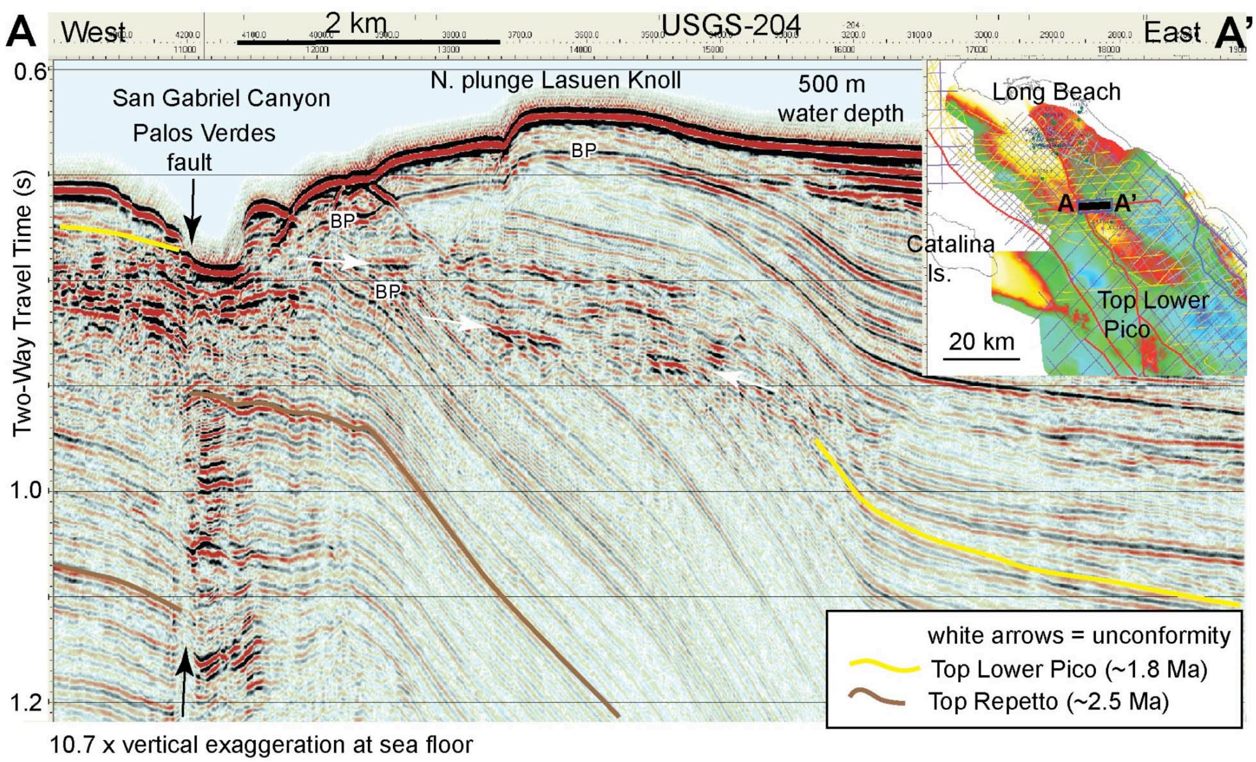

Figure 8: An angular unconformity (white arrows) now is at about 650 m depth. If it is wave eroded, it has since subsided about 550 m. The broad shelf offshore of Long Beach has not subsided and its relative motion above the surrounding subsiding basins, including Los Angeles basin, likely requires a component of slip from regional thrust faults. Data from Sliter et al. (2005). BP=Bubble pulse ("ghost").

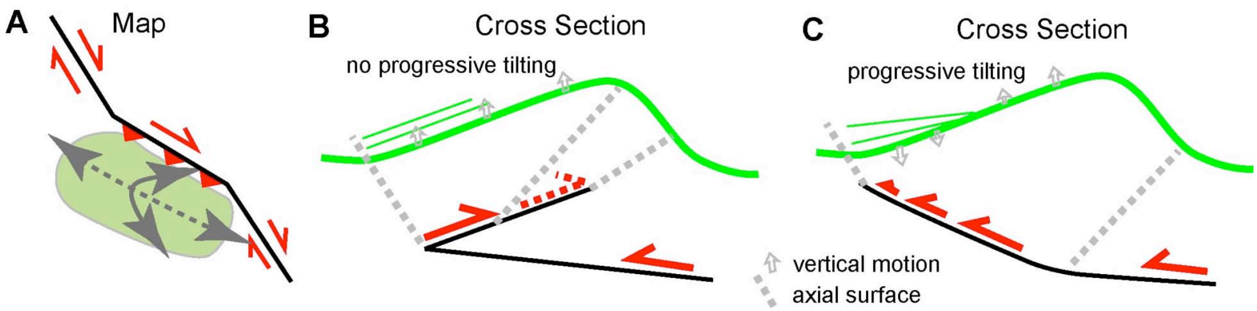

Figure 9: Cartoons similar to models that have been used to explain growth of the Palos Verdes anticlinorium. **"A"** is similar to the restraining segment model of Ward and Valensise (1994), which can explain uplift of Palos Verdes Hills with respect to sea level. The thrust models, **"B"** and **"C"**, can explain the full 70 km-long onshore-offshore Palos Verdes anticlinorium. They also incorporate the strike-slip Palos Verdes fault (not shown). They can be differentiated in part by presence or lack of progressive tilting, which in turn affects the pattern of vertical motions. **"B"** is somewhat similar to Davis et al (1989) and Shaw and Suppe (1996). **"B"** and **"C"** differ in predictions of distribution of slip during an earthquake (length of red slip arrows) and location and directivity of shallow slip.

Progressive tilting of turbidites buried beneath the modern slope from Long Beach to San Clemente City show that if the outer shelf has no vertical motion, the continental slope must be subsiding with rates increasing SW towards the basin (Figs. 7, 9C, 10). This tilting is at a much larger scale than expected from restraining or releasing double bends on strike-slip faults and suggest a contribution from regional blind thrust faults. Such faults have been proposed, but generally with SW dip and wide offshore limbs being back limbs. We propose instead that the gently NE-dipping San Mateo-Carlsbad fault along the base of the slope has been reactivated as a blind oblique thrust fault. According to this model, progressive tilting is thus on the forelimb of the related anticlines.

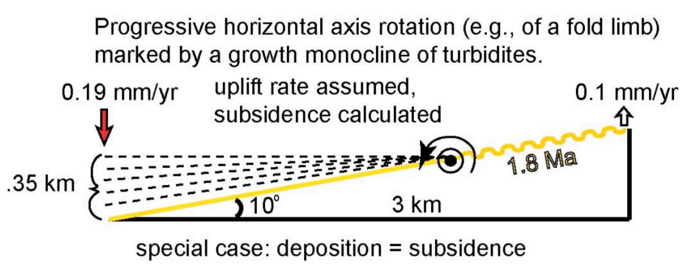

Figure 10: If one knows the dip and age of a horizontally-deposited turbidite, the width of the tilting fold limb, and the vertical motion of one point, it is simple to calculate the vertical motion of other points. Compare to the northeast end of Figure 7.

Continued thermal subsidence is expected after the end Miocene cessation of extension, or after the middle Miocene end of regional extreme extension. A thrust component of activity is required to keep the shelf from subsiding along with the basins. Slip on the Newport-Inglewood fault cannot explain lack of subsidence on both its sides.

4.3: Fault-Fold Models

Thrust Model Predictions

Wide Forelimb models (Fig. 11C)
- Progressive tilting
- Varying rates of vertical motion
- Shallow contraction near base wide limb
- Position of base of wide fold limb controlled by reactivated normal faults that dip beneath that limb.

Wide Backlimb Models (Fig. 11B).
Progressive tilting not required
Constant rates vertical motion on wide limb
Shallow contraction near base narrow limb
Normal faults overridden by thrust wedge.

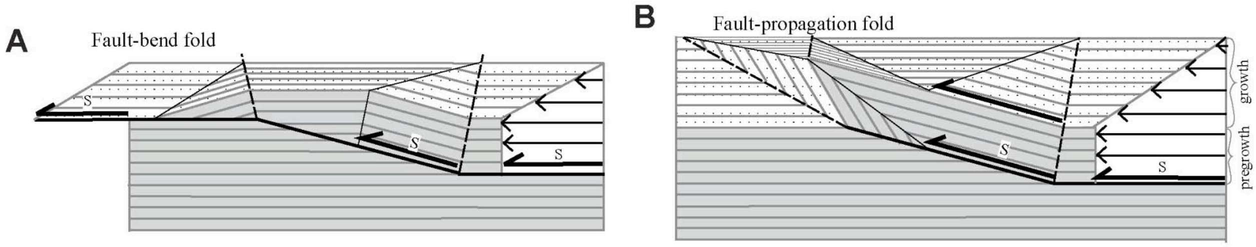

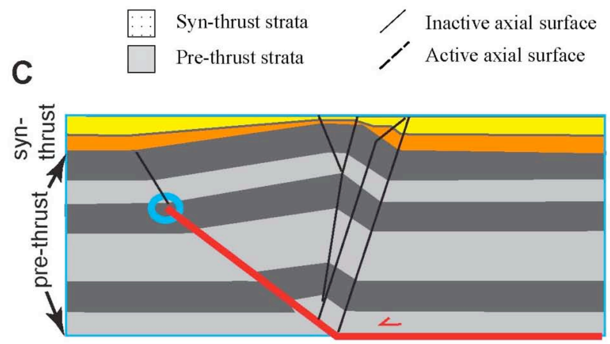

Figure 11: **A**: Fault-bend fold. Slip is >= backlimb width, and backlimbs are slightly wider than fore-limbs (Suppe, 1983). **B**: Fault propagation fold (Suppe and Medwedeff, 1990; Mitra, 1990). Backlimb is wider than forelimb. A and B from Seeber and Sorlien (2000).
C: Displacement gradient fold redrawn from Wickham (1995). Fault tip propagates more slowly than fault slip, or not at all, forcing a broad, progressively-tilting fore-limb that can be much wider than the backlimb.

There is a major difference in estimating earthquake hazard between models that explain anticlinoria as driven by contraction across restraining segments of local strike-slip faults (e.g., Ward and Valensise, 1994) vs. those that require regional thrust faults for part or all of the folding (Davis et al., 1989; Shaw and Suppe, 1996; Sorlien et al., 2009 and manuscript). Whether or not SW-dipping blind thrusts exist in areas above where NE-dipping faults are imaged is also important. Our alternate model is mainly intended to support the existence of a regional thrust system rooted beneath Los Angeles by better matching tilts, locations of shallow contraction, and the history of vertical motions. We also propose that the Newport Beach to San Clemente slope is a progressively-tilting forelimb and that blind thrust slip on the northwest San Mateo-Carlsbad fault (northwest Oceanside thrust) contributes to uplift of the San Joaquin Hills.

The interpretations that include faults dipping away from the mainland all use ramp-flat (kink) models, fault bend folds and/or fault propagation folds. In these models the backlimb is broader than the forelimb (Figs. 11A, 11B). Where anticlines are asymmetric, the broad limb is interpreted as the backlimb, with the fault dipping in that direction. However, various models that include broad progressively tilting forelimbs have been published (example: Figure 11C; Wickham, 1995). The ubiquity of progressively-tilted forelimbs along the southern California margin may be related to the fact that most large thrust-separation faults are reactivated Miocene normal-separation faults (Figures 2B, 3; Yeats and Beall, 1991; Seeber and Sorlien, 2000; Sorlien et al., 2006; Schindler et al., 2007; Schindler, 2010).

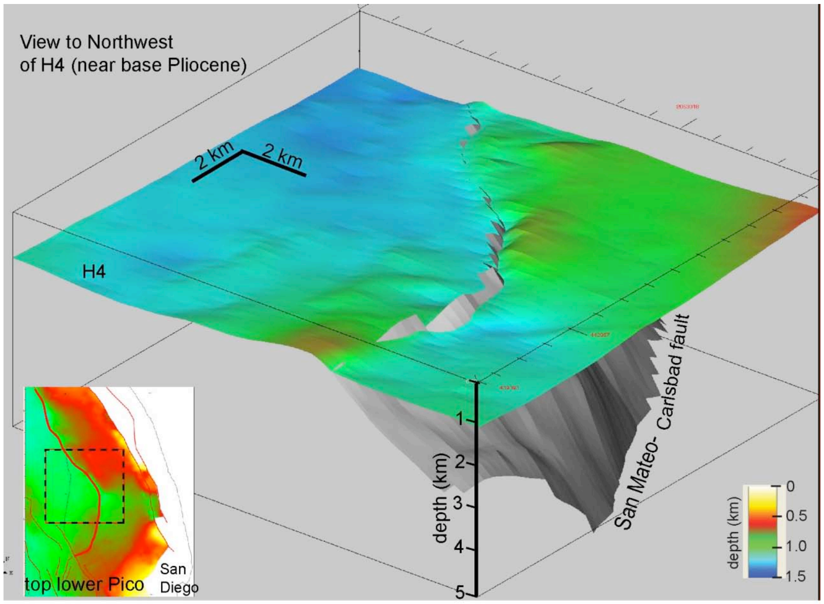

Figure 12: oblique view to northwest of the San Mateo-Carlsbad fault (gray) through the northern bend of its releasing segment. The horizon is H4 (near base Pliocene), and the reversal from reverse to normal separation through the bend is obvious. Dozens of seismic reflection profiles located within this volume (Fig. 3) were used to construct this part of the grid. The inset giving the location of this volume(dashed square) includes a structure-contour of top Lower Pico.

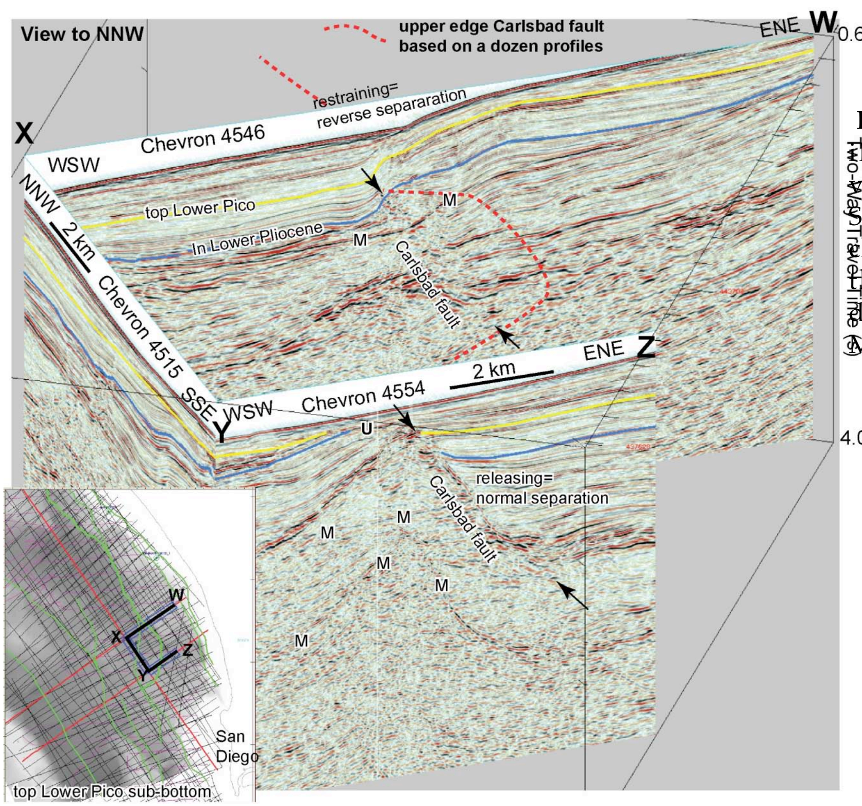

Figure 13. Fence diagram, illustrating how the sense of vertical displacement along the San Mateo-Carlsbad Fault changes from normal to reverse through a bend in that fault (red dash). U: Unconformity M: Multiple

local strike and apparent dip (San Mateo-Carlsbad), structural relief (top Lower Pico, yellow, within 1 km footwall, 4 km hanging-wall)

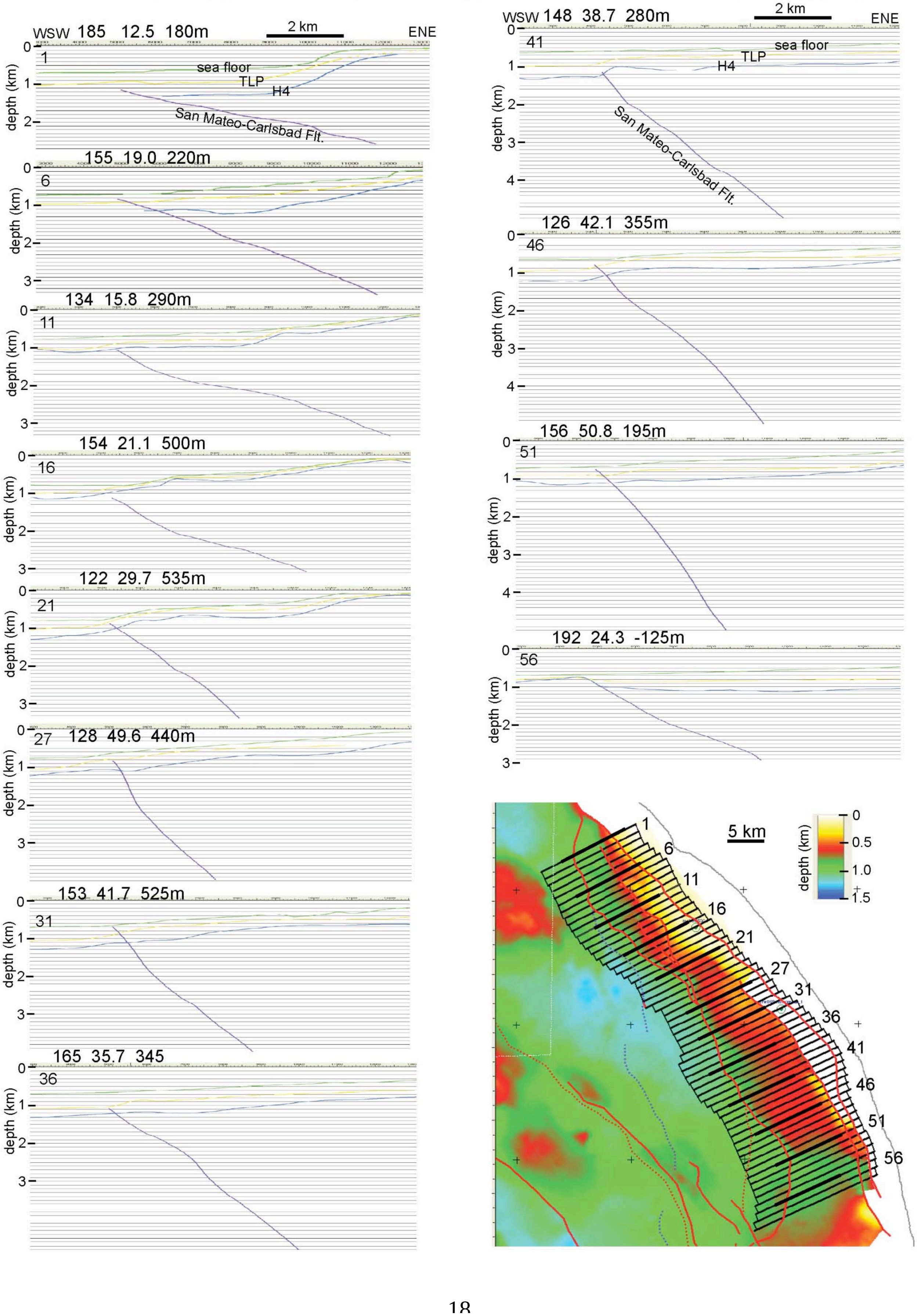

Figure 14: (previous page): ENE-WSW cross sections through the depth-converted sea floor, horizons, and fault grid, located by heavy lines on map at lower right. Map is of top Lower Pico. A ten km part of every fifth cross section is displayed. Numbers above sections are strike, dip, and structural relief of top Lower Pico (yellow) in meters within 1 km of the upper tip of the fault in its footwall and 4 km in its hanging-wall.

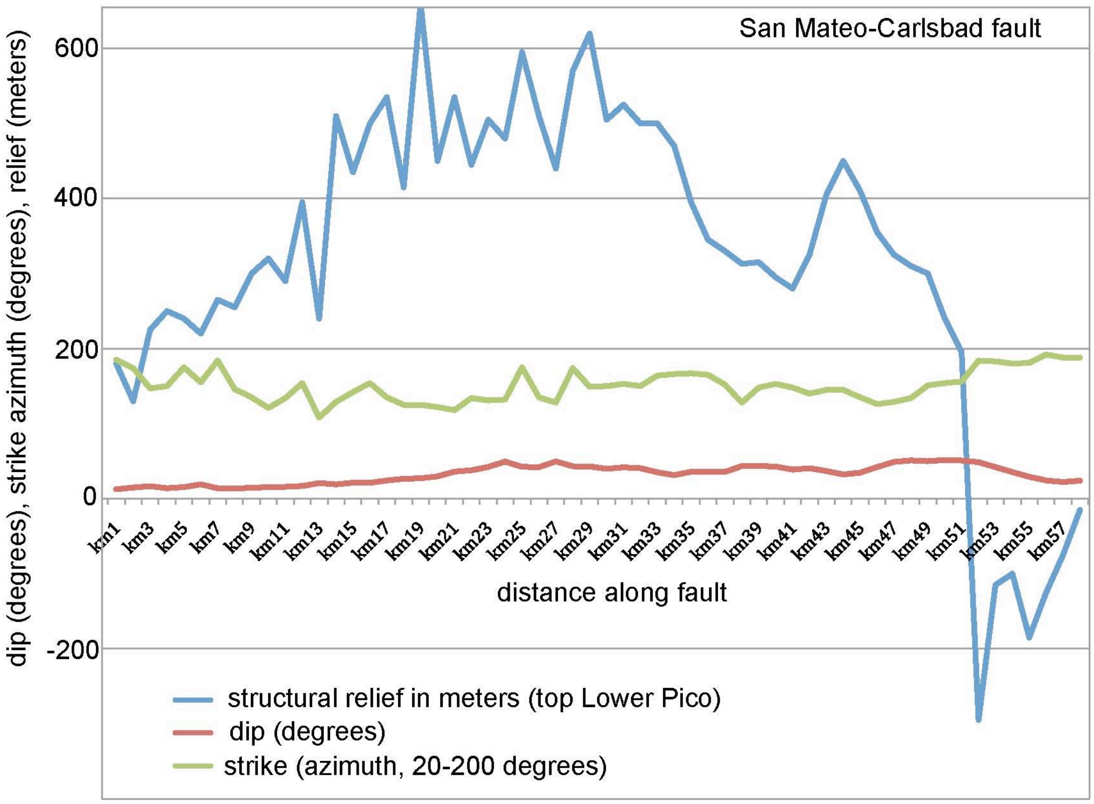

Figure 15: comparison of strike and dip of the San Mateo-Carlsbad fault to structural relief of top Lower Pico within 1 horizontal km of the upper edge of the fault in its footwall and within 4 km in its hanging-wall. The vertical graph scale is the same for all 3 curves, even though it includes both angles in degrees and relief in meters. Relief increases from left to right as strike azimuth decreases (becomes more E-W), and vice-versa. Structural relief also increases as fault dip increases. The reversal from reverse to normal separation at km 52 is consistent with right-lateral slip.

4.4: Slip on the San Mateo-Carlsbad fault

The general pattern of fault strike vs. structural relief is suggestive of right-lateral slip on the southern part of this fault. Figure 16 shows that as the fault strike azimuth decreases (becoming more E-W, smaller values = down on graph), the structural relief increases. If right-lateral slip occurs on this fault a more E-W strike is restraining and structural relief should be larger. In particular, the abrupt change from reverse to normal separation within 2 km in the bend into a N-S segment further supports right-lateral slip (Figs. 12, 13, 14, 15). The relation of vertical motions to slip on non-vertical strike-slip faults has been examined in Santa Monica Bay, California (Sorlien et al., 2006) and for the North Anatolian fault near Istanbul, Turkey (Seeber et al., 2006).

A simple trigonometric model is used to estimate slip direction and slip magnitude on the San Mateo Carlsbad fault. This preliminary model will be refined for the thesis of B. Campbell and eventual publication. It assumes vertical motion is due to simple transport (obliquely) up or

down a ramp of a given apparent dip. We model slip of the hanging wall with respect to the footwall towards 240, 220, 200, and 180 degrees. 240 degrees is perpendicular to the average strike of the modeled 58 km-long segment of the fault. 180 degrees is oblique right-reverse to the average strike but is pure right-lateral within part of the bend. The best average fit between measured and modeled structural relief is given by a slip of 1 km +/- 0.5 km towards due south. The error can be decreased by simply running smaller slip increments; measurement,

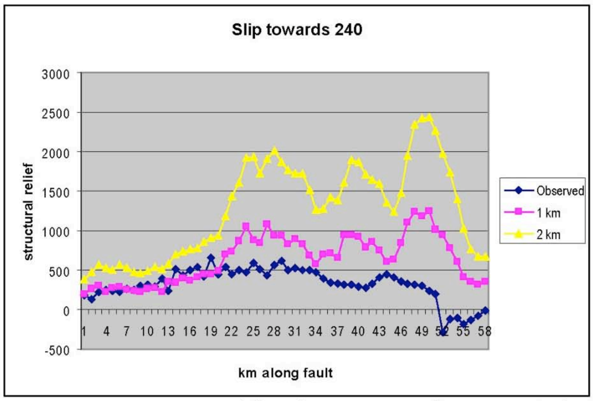

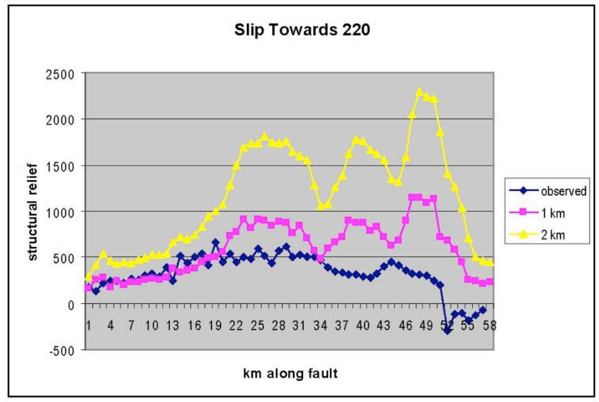

blue is measured, magenta is 1 km slip, yellow is 2 km slip

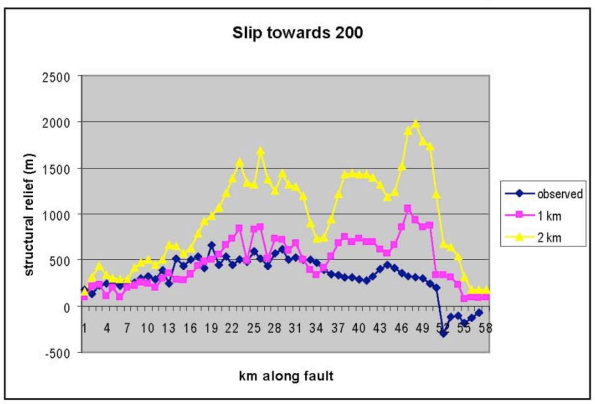

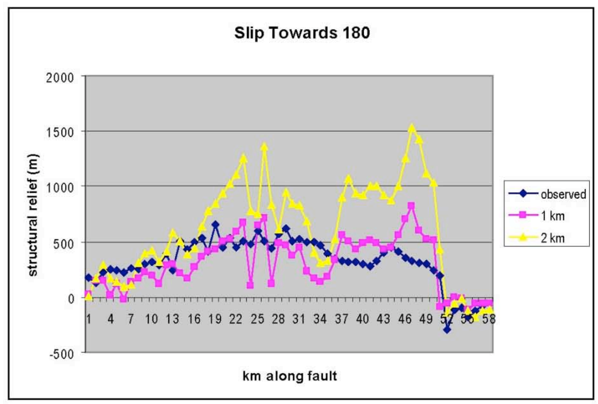

Figure 16: Graphs of modeled vs. measured structural relief calculated using equation 1. This is for a 58 km-long segment of the San Mateo-Carlsbad fault. This model structural relief (SR) at any point along the fault can be computed from the geometry of the fault over the slip, assigned to be in the x-direction.

$$\textbf{(1)}\ SR=\Sigma_i 1km*\sin(\alpha_i)*\tan(\delta_i)$$

Where α is the angle between the local slip vector and local fault strike and δ is fault dip. The slip direction of the hanging-wall, fault strike, and fault dip are used for each 1 km bin along the fault to calculate increase in structural relief for rock passing through each bin. The curve for 2 km slip (yellow) adds the calculated increase in structural relief for the bins 1 and 2 km upstream (north). The dark blue curve is the measured structural relief of the top Lower Pico horizon within 1 km horizontally in the footwall and 4 km in the hanging wall of the fault tip.

interpretation, and depth conversion errors are not included. Measurement errors are about 1 degree for angles and 20 m for relief, and depth conversion errors are likely less than 10% but will be compared to the 3D velocity model in progress. Additional slip directions will be modeled including slip towards the SSE. The northern part of the fault is well-fit by pure thrust slip (towards 240). It is thus also possible that a right-lateral component of slip is transferred from the Newport-Inglewood fault to the San Mateo-Carlsbad fault towards the south.

The continuity of kinematics is supportive of our interpretation of one continuous fault rather than discontinuous segments. Structural relief on the top Lower Pico (TLP) was modeled. This horizon is about 1.8 Ma near the Beta oil field of San Pedro Shelf (Blake, 1991). Our long regional correlations through multiple paths could allow our surface to be time-transgressive. However, major onlap is generally onto unconformities above TLP. We speculate that a reasonable age range for TLP in the area that we modeled is 1.5 to 2 Ma. The long-term average slip rate would then be 0.67 to 0.5 mm/yr (+/- 50% since we only modeled slip in 1 km increments). However, Covault and Romans (2009) interpreted strata just above our TLP to be about 160,000 years old. If they are correct and the TLP or an unconformity just above it do not represent a major hiatus, then the slip rate on the San Mateo-Carlsbad fault would be as much as 6 mm/yr (+/- 50%). Stratigraphic information from the Caldrill 68 coreholes displayed on F-F' in Figure 5 could settle this uncertainty. Any data on these coreholes existing in U.S. Minerals Management Service files is available to the U.S.G.S. The coreholes are otherwise proprietary, and an effort by C. Sorlien in ~1995 to have them released was unsuccessful. We have renewed the request to have this valuable data set released.

4.5: Summary

Products from this study include new 3D representations of faults and stratigraphic horizons, and new estimates of fault slip rates and slip directions for the San Mateo-Carlsbad fault. Rare major (oblique) thrust earthquakes on either the northwest San Mateo-Carlsbad fault or the San Pedro Escarpment-Compton thrust system might be expected to generate tsunamis with very little warning time due to proximity of the source to the coast. The basic geometric information provided in this study will allow maximum credible earthquake magnitudes to be calculated by others. Additional segments of non-sub-vertical faults will be gridded and depth converted for the thesis of B. Campbell. The digital fault and stratigraphic representations will be provided to the SCEC Community Fault Model, to U.S.G.S. scientists, and to the U.S. Minerals Management Service, and can be used for seismic source characterization including tsunami modeling. Three-dimensional graphical views and animations will be published and/or put online allowing earth scientists who do not specialize in such work to better understand the regional structure

5: Other Information and Data availability

To date 5 abstracts have been accepted for this project: Sorlien et al. 2009, Sorlien et al. 2010a, b; Campbell et al., 2009, Alward et al., 2009. A University of Missouri Masters thesis is under preparation by B. Campbell. Much of C. Sorlien time during the NEHRP funding period was for completing of interpretations and revisions related to resubmission of a manuscript on Palos Verdes anticlinorium, which was ultimately rejected and will be resubmitted elsewhere (Sorlien et al., manuscript).

Brian Campbell was available at no cost to this USGS-NEHRP project, and was trained in all the techniques described here. Leonardo "Nano" Seeber was not supported by this project. The southern part of the Palos Verdes anticlinorium was part of this USGS-NEHRP supported project, while work by C. Sorlien on areas farther north was supported by the Southern California Earthquake Center in grants made in 2008 and earlier. Digital gridded horizon maps and the San Mateo-Carlsbad fault grid from this project have been offered to the U.S. Minerals Management Service and to U.S. Geological Survey geologists/geophysicists working on this region. The slip model in Figure 16 is preliminary and will be refined with more slip directions and smaller slip increments. The strike of the San Mateo – Carlsbad fault will be measured from its grid at 2 or 3 km depth rather than at its upper tip. A 3D velocity model based mainly on industry stacking velocities for seismic reflection data is planned. The fault grid, and any future depth-converted representations of other faults, will be provided to the SCEC Community Fault Model. The gridded horizons will be provided to the SCEC CFM upon publishing this work, and as supplemental data to a publication resulting from this study. Due to budget problems at

the University of California, C. Sorlien's home institution, the Institute for Crustal Studies, is merging with another research Institution. The new Earth Research Institute internet name is not yet available for a web site for data from this study, but the web address will probably be **http://research.eri.ucsb.edu/sorlien-usgs08HQGR0103/**. The full resolution version of this report will be available there or by email request. Later, links will be added to products and publications, and digital horizon and fault grids. Information can be obtained from C. Sorlien at **chris@crustal.ucsb.edu**. This email address will become sorlien@eri.ucsb.edu in future years. The 2D fault traces are easily exported in geographic coordinates and will be supplied on request.

6: Acknowledgments

Seismic Micro Technology donated "The Kingdom Suite" interpretation software used in this study. The authors acknowledge WesternGeco, Chevron, and the US Geological Survey for providing the seismic reflection data for the purpose of this research. WesternGeco, Chevron, and the USGS do not warrant the use of these data, nor make any claims or guarantees as to the accuracy of the data identification, acquisition parameters, processing methods, navigation or database entries. Paradigm donated licenses to Gocad, which was used to create Figure 1B. Kris Broderick, Mike Fisher, Ray Sliter, Bruce Luyendyk, and Bill Normark were involved in work near Palos Verdes anticlinorium. William Alward, a graduate student at University of Missouri, was involved in interpretations in the western part of the study area, and loaded a substantial amount of data there and elsewhere. Marie-Helene Cormier is the thesis advisor of Brian Campbell, produced the bathymetric grid used in the southern half of the study area, and provided an edit. Sorlien worked with Mark Legg and Craig Nicholson in the early 1990s on structure of the southern part of this study area, and have continued discussions of Borderland geology. Greg De Hoogh provided expertise on use of Kingdom Suite, and with Craig Nicholson, we mutually benefited from comparisons of Inner and Outer Borderland structure. Drew Mayerson and Frank Victor of the U.S. Minerals Management Service provided the digital public well logs. Holly Ryan, Jamie Conrad, and others at USGS, as well as Jake Covault of Chevron are acknowledged for interesting discussions of structure and stratigraphy.

7: REFERENCES

Alward, W. S., C. C. Sorlien, R. L. Bauer, and B. A. Campbell, 2009, Mergence of the Palos Verdes, San Pedro Basin, and San Diego Trough fault zones: A 220+ km-long fault system, Southern California Earthquake Center Annual Meeting, Proceedings and Abstracts v. XIX poster 2-024, p. 263.

Blake, G. H., 1991, Review of the Neogene biostratigraphy and stratigraphy of the los Angeles Basin and implications for basin evolution, in K.T. Biddle, ed., Active Margin Basins, AAPG Memoir 52, American Association of Petroleum Geologists, Tulsa, p. 135-184

Bohannon, R. G. and E. L. Geist, 1998, Upper crustal structure and Neogene tectonic development of the California continental borderland, Geological Society of America Bulletin, v. 110, p. 779-800

Brankman, C. M., and J. H. Shaw, (2009), Structural geometry and slip of the Palos Verdes fault, southern California: Implications for earthquake hazards, *Bull. Seism. Soc. Amer., 99*, 1730-1745.

Broderick, K.G., (2006), Giant blind thrust faults beneath the Palos Verdes Hills and western Los Angeles Basin, California: Mapping with seismic reflection and deep drilling data, unpublished M.S. thesis, 68 pp., University of California, Santa Barbara, Santa Barbara, California.

Campbell, B. A., C. C. Sorlien, M.-H. Cormier, and W. S. Alward, 2009, Quaternary deformation related to the 3D geometry of the Carlsbad fault, offshore San Clemente to San Diego, Southern California Earthquake Center Annual Meeting, Proceedings and Abstracts v. XIX poster 2-025, p. 263-264.

California Division Oil, Gas, and Geotherm Resources, (1992). California Oil & Gas Fields, Volume II: Southern, Central Coastal, and Offshore California, Pub. TR11.
Conrad, J. E., H. F. Ryan, and R. W. Sliter, 2008, Active strike-slip faulting in the Inner Continental Borderland, southern California: Results from new high-resolution seismic reflection data, Eos Trans. AGU, 89(53), Fall Meet. Suppl., Abstract T41A-1934.
Covault, J. A. and B. W. Romans (2009). Growth patterns of deep-sea fans revisited: Turbidite-system morphology in confined basins, examples from the California Borderland, Marine Geology 265(1-2): 51-66.
Crouch, J. K., and J. Suppe (1993), Late Cenozoic tectonic evolution of the Los Angeles basin and inner California borderland: A model for core complex-like crustal extension, *Geol. Soc. Am. Bull.* 105, 1415-1434.
Dartnell, P., and J. V. Gardner (1999), Sea-Floor Images and Data from Multibeam Surveys in S.an Francisco Bay, Southern California, Hawaii, the Gulf of Mexico, and Lake Tahoe, California-Nevada, *U.S. Geol. Surv. Digital Data Series* DDS-55 Version 1.0.
Davis, T. L., J. Namson, and R. F. Yerkes (1989), A cross section of the Los Angeles Area: Seismically active fold and thrust belt, the 1987 Whittier Narrows earthquake, and earthquake hazard, *J. Geophys. Res*, *94*, 9644-9664.
Fisher, M. A., W. R. Normark, V. E. Langenheim, A. J. Calvert , and R. W. Sliter, (2004), The offshore Palos Verdes fault zone near San Pedro, southern California, *Bull. Seism. Soc. Amer.*, v. 93 p. 1955-1983.

Grant, L. B., K. J. Mueller, E. M. Gath, H. Cheng. R. L. Edwards, R. Munro, G. L. Kennedy, 1999, Late Quaternary uplift and earthquake potential for the San Joaquin Hills, southern Los Angeles basin, California, Geology, v. 27, p. 1031-1034
Grant, L. B., L. J. Ballenger, and E. E. Runnerstrom, 2002, Coastal uplift of the San Joaquin Hills, southern Los Angeles basin, by a large earthquake since A.D. 1635, Bulletin of Seismological Society of America, v. 92, p. 590-599
Grant, L. S., and P. M. Shearer, 2004, Activity of the offshore Newport-Inglewood Rose Canyon fault zone, coastal southern California, from relocated microseismicity: Bulletin of the Seismological Society of America, v. 94, p 747-752.
Hart, P. E. and J. R. Childs, 2005, National archive of marine seismic surveys (NAMSS): Status report on U. S. Geological Survey program providing access to proprietary data, *Eos Trans. AGU*, *86*(18), Jt. Assem. Suppl., Abstract S41A-10, http://walrus.wr.usgs.gov/NAMSS/.
Jennings, C. W., 1994, Fault activity map of California and adjacent areas with locations and ages of recent volcanic eruptions, California Division of Mines and Geology, Geologic Data Map no. 6 scale 1:750,000
Jennings, C. W, W. A. Bryant, and G. Saucedo, 2010, Fault activity map of California, California Geological Survey
http://www.consrv.ca.gov/cgs/cgs_history/PublishingImages/FAM_750k_MapRelease_page.jpg
http://www.quake.ca.gov/gmaps/FAM/faultactivitymap.html
Legg, M. R., V. O. Wong, F. V. Suarez., 1991, Geologic structure and tectonics of the inner Continental Borderland of northern Baja California, in The Gulf and Peninsular Province of the Californias, J. P. Dauphin and B. R. T. Simoneit, American Association of Petroleum Geologists Memoir 47, Tulsa, Oklahoma, p. 145-177.
Legg, M. R., 1991, Developments in understanding the tectonic evolution of the California Continental Borderland, in: Osborne, R. H., ed., Shepard Commemorative Volume, From Shoreline to Abyss, Society of Economic Paleontologists and Mineralogists, Special Publication no. 46, p. 291-312
McNeilan, T. W., T. K. Rockwell, and G. S. Resnick, 1996, Style and rate of Holocene slip, Palos Verdes fault, southern California, Journal of Geophysical Research, v. 101, p. 8317-8334
Mitra, S., 1990, Fault-propagation folds: geometry, kinematic development, and hydrocarbon traps, Americam Association of Petroleum Geologists v. 74, no. 6, p. 921-945

Nardin, T. R., and T. L. Henyey (1978). Pliocene-Pleistocene diastrophism of Santa Monica and San Pedro shelves, California Continental Borderland, *Amer. Assoc. Petroleum Geol. Bull.* 62, 247-272.

Nicholson, C., C. C. Sorlien, and M. R. Legg, 1993, Crustal imaging and extreme Miocene extension of the inner California Continental Borderland, Geological Society of America Abstracts With Programs, vol. 25, no. 6

C. Nicholson, C. C. Sorlien, M. J. Kamerling, M. R. Legg, 1996, Crustal Imaging Along the southern California margin: Miocene Extension, Rotation, and Tectonic Inversion Related to an Evolving Transform System, EOS, (Trans. AGU), v. 77, no. 46, p.F738

Normark, W. R., D. J. W. Piper, B.W. Romans, J.A. Covaults, P. Dartnell, and R.W. Sliter (2009). Submarine canyon and fan systems of the California Continental Borderland. Earth Science in the Urban Ocean: The Southern California Borderland. H. J. Lee and W. R. Normark. Boulder, CO, The Geological Society of America. Special Paper 454: 141-168Pinter, N., C. C. Sorlien, and A. T. Scott (2003), Fault-related fold growth and isostatic subsidence, California Channel Islands, *Am. J. Science*, 303, 300-318.

Plesch, A, J. H. Shaw, C. Benson, W. A. Bryant, S. Carena, M. Cooke, J. Dolan, G. Fuis, E. Gath, L. Grant, E. Hauksson, T. Jordan, M. Kamerling, M. Legg, S. Lindvall, H. Magistrale, C. Nicholson, N. Niemi, M. Oskin, S. Perry, G. Planansky, T. Rockwell, P. Shearer, C. Sorlien, M. P. Suss, J. Suppe, J. Treiman, and R. Yeats, Community Fault Model (CFM) for southern California, Bulletin of the Seismological Society of America, V. 97, p. 1793-1802, DOI: 10.1785/0120050211

Ponti, D.J., and K.D. Ehman, A 3-D sequence-based structural model for the Quaternary Los Angeles Basin, California, SCEC annual meeting, Proceedings and Abstracts, volume XIX, Abstract 2-023, Sept. 12-16 2009.

Rigor, A. W., 2003, Structure and deformation of the Palos Verdes fault in San Pedro Bay, California, Master's thesis, San Diego State University, 67 pages.

Rivero, C., J. H. Shaw, and K. Mueller, 2000, Oceanside and Thirtymile Bank blind thrusts: Implications for earthquake hazards in coastal southern California, Geology, v. 28, p. 891-894.

Ryan, H. F., M. R. Legg, J. E. Conrad, and R. W. Sliter, 2009, Recent faulting in the Gulf of Santa Catalina: San Diego to Dana Point, in H.J. Lee and W. R. Normark, eds., Earth Science in the Urban Ocean: The Southern California Continental Borderland: Geological Society of America Special Paper 454, p. 291-315, doi: 10.1130/2009.2454(4.5).

Schindler, C. S., 2010, 3D fault geometry and basin evolution in the northern Continental Borderland offshore Southern California, M.S. Thesis, California State University, Bakersfield, 41 pages. http://www.csub.edu/library/thesis/schindler_c_geo_w10.pdf

Schindler, C. S., C. Nicholson, and C. Sorlien, 2007, 3D fault geometry and basin evolution in the northern Continental Borderland offshore southern California, *Eos Trans. AGU, 88*(52), Fall Meet. Suppl., Abstract T43A-1100.

Seeber, L, and C. C. Sorlien (2000), Listric thrusts in the western Transverse Ranges, California, *Geol. Soc. Amer. Bull.* 112, 1067-1079.

Seeber, L., M.-H. Cormier, C. McHugh, O. Emre, A. Polonia, and C. Sorlien, 2006, Rapid subsidence and sedimentation from oblique slip near a bend on the North Anatolian transform fault in the Marmara Sea, Turkey, Geology 34 p. 933-936; doi: 10.1130/G22520A.1

Shaw, J. H., and J. Suppe (1996), Earthquake hazards of active blind-thrust faults under the central Los Angeles basin, California, *J. Geophys. Res., 101*, 8623-8642.

Sliter, R. W., W. R. Normark, and C. E. Gutmacher (2005), Multichannel seismic-reflection data acquired off the coast of southern California-Part A 1997, 1998, 1999, and 2000, *U. S. Geological Survey Open-File Report 2005-1084*, http://pubs.usgs.gov/of/2005/1084/index.html.

Sorlien, C. C., K. G. Broderick, L. Seeber, B. P. Luyendyk, M. A. Fisher, R. W. Sliter, and W. R. Normark, Offshore Los Angeles Thrust-folding: Pliocene-Quaternary Evolution of Palos Verdes Anticlinorium, California, unpublished manuscript.
Sorlien, C. C., B. A. Campbell, W. S. Alward, L. Seeber, M. R. Legg, and M.-H. Cormier, 2009, Transpression in strike-slip restraining segments vs. regional thrusting in the Inner California Continental Borderland, Southern California Earthquake Center Annual Meeting, Proceedings and Abstracts v. XIX poster 2-026, p. 264-265.
Sorlien, C. C., M. J. Kamerling, L. Seeber, and K. G. Broderick (2006), Restraining segments and reactivation of the Santa Monica–Dume–Malibu Coast fault system, offshore Los Angeles, California, *J. Geophys. Res.*, *111*, doi:10.1029/2005JB003632.
Sorlien, C., and L. Seeber, 2010, Reactivation, fault-fold models and vertical motions, Long Beach to San Clemente, California, Annual Report to Southern California Earthquake Center, 5 pages.
Sorlien, C. C., L. Seeber, B. A. Campbell, 2010a, Quaternary subsidence in the Inner California Continental Borderland: Echo of Miocene crustal thinning and thrust-folding of the near-shore slope, Pacific Section AAPG and GSA Cordilleran joint meeting, Anaheim California, May 2010
Sorlien, C. C., et al. (REPONS Scientific Team), 2010b, Thrust-reactivated normal faults and thrust-folding California Borderland and Haiti, Pacific Section AAPG and GSA Cordilleran joint meeting, Anaheim California, May 2010
Suppe, J., (1983), Geometry and kinematics of fault-bend folding, *Am. J. Science*, *283*, 684-721.
Suppe, J., and D. A. Medwedeff, (1990), Geometry and kinematics of fault-propagation folding, *Eclogae geol. Helv.*, *83*, 409-454.
Tolmachoff, W., 1993, Linear velocity functions and the effects of mentors on the oil industry, Pacific Petroleum Geologist Newsletter, no. 2, Pacific Section, American Association of Petroleum Geologists, p. 4-5
U. S. Geological Survey and Southern California Earthquake Center, Scientists of (1994), The magnitude 6.7 Northridge, California earthquake of 17 January, 1994, *Science* 266, 389-397.
Vedder, J. G. (1990), Maps of California Continental Borderland showing compositions and ages of samples acquired between 1968 and 1979, *U. S. Geol. Surv. Misc. Field Studies Map* MF-2122**.**
Ward, S. N., and G. Valensise, (1994), The Palos Verdes terraces, California: Bathtub rings from a buried reverse fault, *J. Geophys. Res.*, *99*, 4485-4494.
Wickham, J., (1995), Fault displacement-gradient folds and the structure at Lost Hills, California (U.S.A.), *J. Structural Geology*, *191*, 1293-1302.
Wright, T. L. (1991), Structural geology and tectonic evolution of the Los Angeles Basin, California, in *Active Margin Basins*, edited by K.T. Biddle, AAPG Memoir **52**, 35-134.
Yeats, R. S., and J. M. Beall, (1991), Stratigraphic controls of oil fields in the Los Angeles basin, A guide to migration history, in *Active Margin Basins*, *AAPG Memoir 52*, edited by K.T. Biddle, pp. 221-235, American Association of Petroleum Geologists, Tulsa, Oklahoma.